

# Simulation des figures de diffraction et des images haute résolution HRTEM et HRSTEM, effets des aberrations.

UMET, UMR CNRS 8207-Université de Lille I

Lille

Octobre 2015

Pierre Stadelmann  
JEMS-SAAS  
CH-3906 Saas-Fee  
Switzerland

October 6, 2015

- ▶ **Why?**
- ▶ **How?**
  - ▶ **Models.**
  - ▶ **Approximations.**
  - ▶ **Methods.**
  - ▶ **Detector.**
  - ▶ **Software.**

We will consider 3 structures and show that image simulation helps understand HRTEM images.

- ▶ **Simple structure:** Co
- ▶ **More complicated structure:**  $MgZn_2$
- ▶ **Complicated structure:**  $Cr_3Ni_5Si_2$

# Simple structure: Co

When simple structures are imaged, image simulation may not be necessary at all. For example looking at Co (P63/mmc, magnetic!), model structure, projected potential, SAED, HRTEM are simple (and straight forward to interpret?):

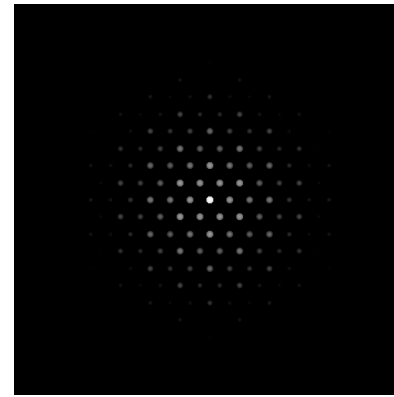
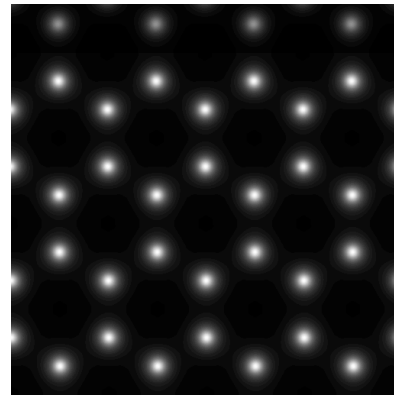
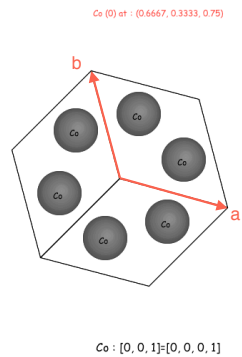


Figure: Model structure Cobalt, [001].

Figure: Projected potential Co [001]

Figure: Selected Area Electron Diffraction (SAED) Co [001].

Figure: HRTEM image Co [001], Titan negative Cs.

# More complicated structure: $MgZn_2$

When moderately complicated structures are imaged, image simulation may still not be necessary. For example looking at  $MgZn_2$  (P63/mmc), model structure, projected potential, SAED, HRTEM are simple (SAED straight forward to interpret?):

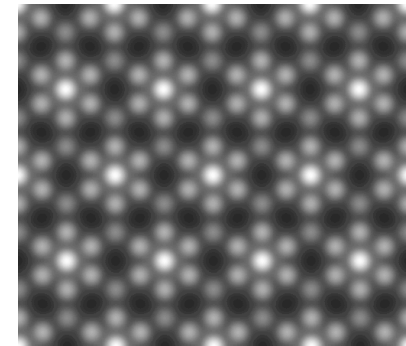
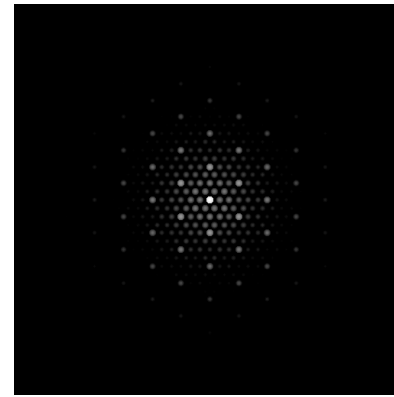
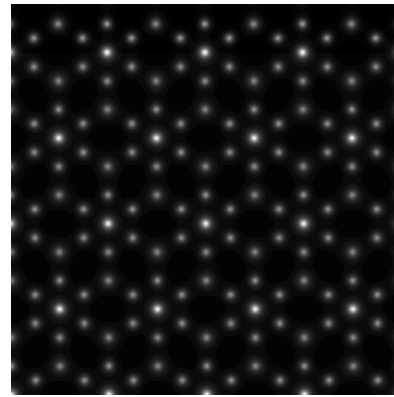
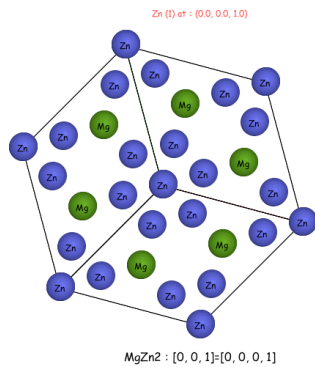


Figure: Model structure  $MgZn_2$ , [001].

Figure: Projected potential  $MgZn_2$  [001]

Figure: Selected Area Electron Diffraction (SAED)  $MgZn_2$  [001].

Figure: HRTEM image  $MgZn_2$  [001], Titan negative Cs.

# Co observed in $[120]$ projection (Weber notation $[10-10]$ )

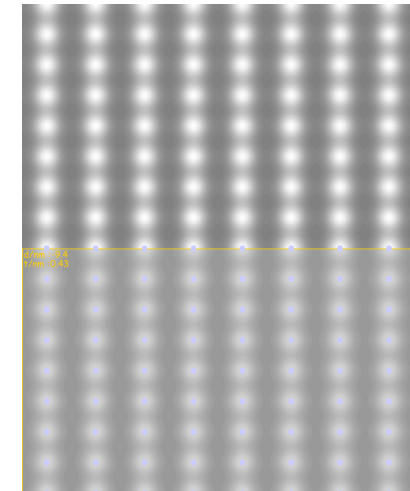
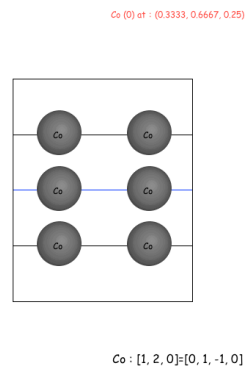


Figure: Model structure Cobalt,  $[120]$ .

Figure: Projected potential Co  $[120]$

Figure: Selected Area Electron Diffraction (SAED) Co  $[120]$ .

Figure: HRTEM image Co  $[120]$ , Titan negative Cs.

# $MgZn_2$ observed in $[120]$ projection (Weber notation $[10-10]$ )

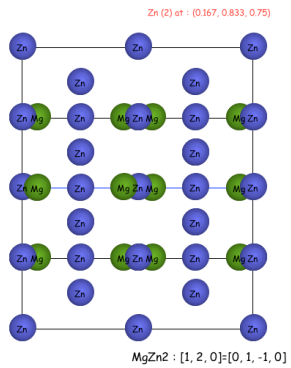


Figure: Model structure  $MgZn_2$ ,  $[120]$ .

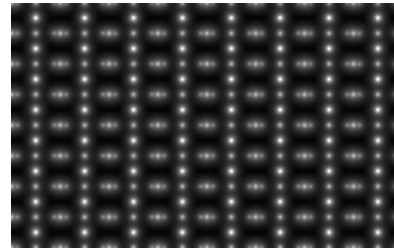


Figure: Projected potential  $MgZn_2$   $[120]$

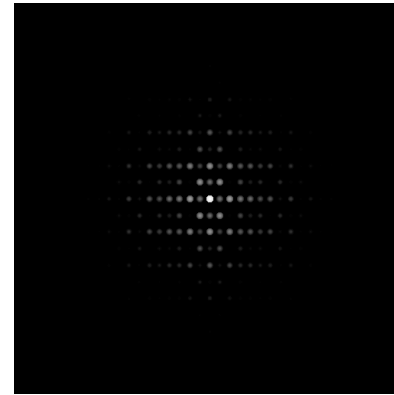


Figure: Selected Area Electron Diffraction (SAED)  $MgZn_2$   $[120]$ .

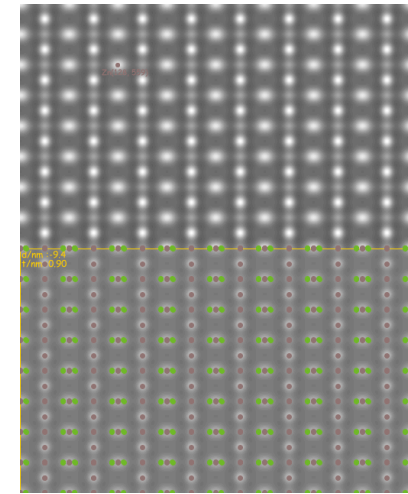


Figure: HRTEM image  $MgZn_2$   $[120]$ , Titan negative Cs.

# Complicated structure: $Cr_3Ni_5Si_2$ observed in [001] projection

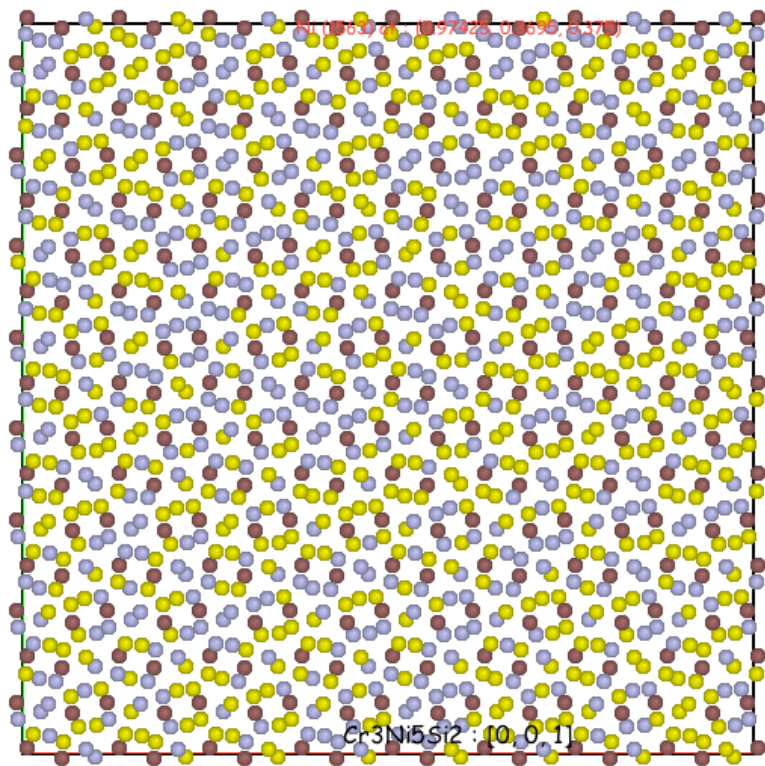


Figure: Model structure  $Cr_3Ni_5Si_2$ , [001].

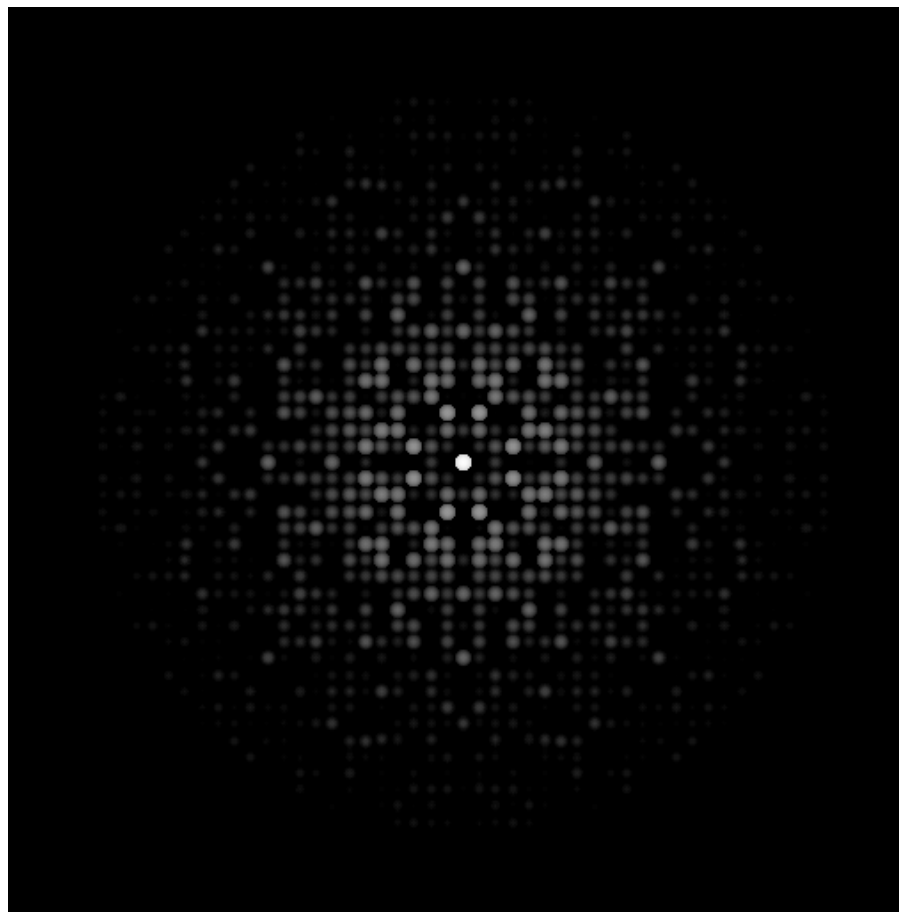


Figure: Selected Area Electron Diffraction (SAED)  $Cr_3Ni_5Si_2$  [001]



# $Cr_3Ni_5Si_2$ observed in $[001]$ projection

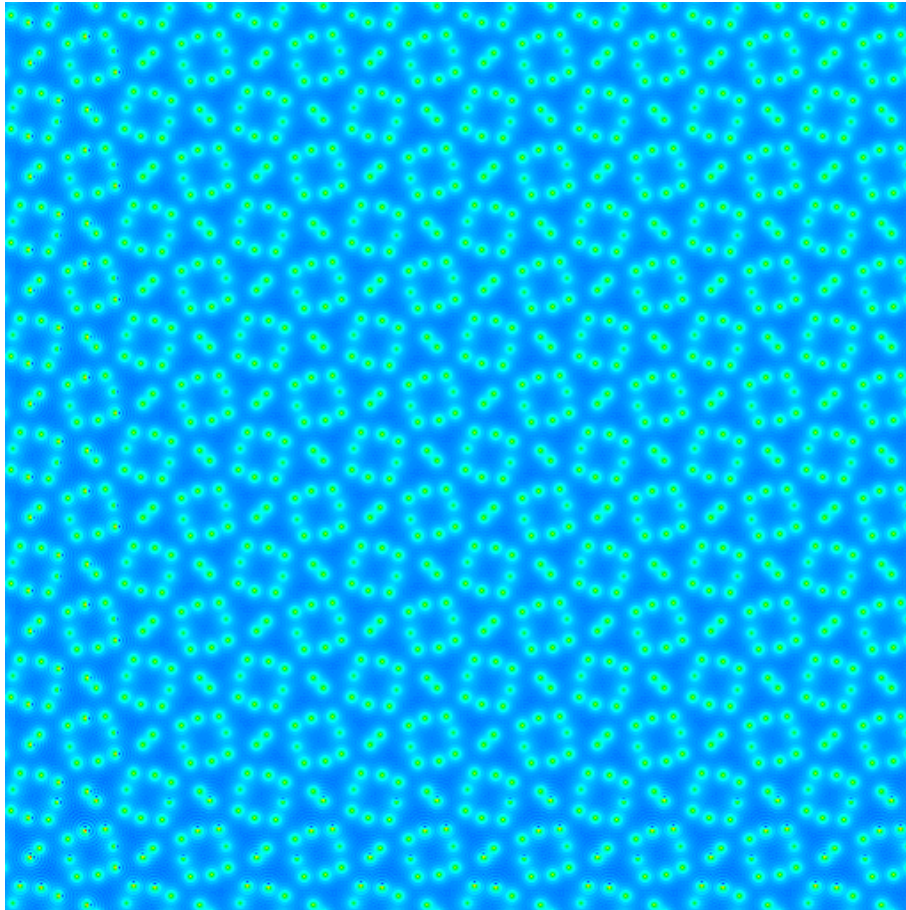


Figure: Projected potential  $Cr_3Ni_5Si_2$   $[001]$ .

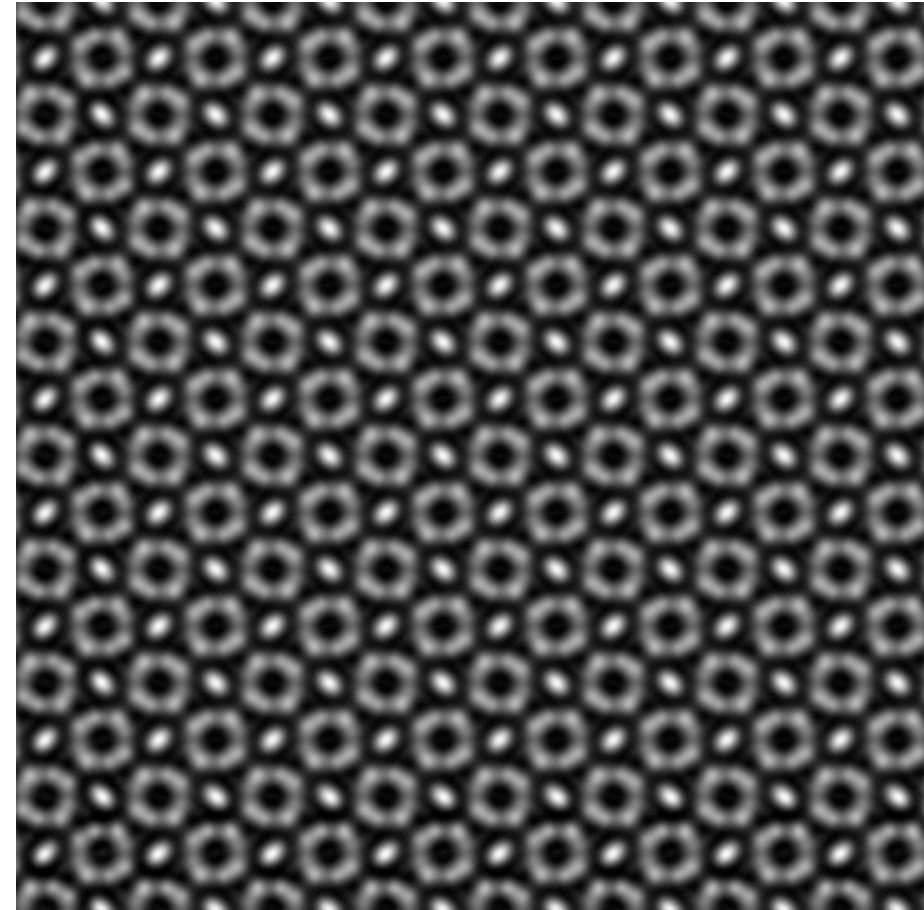


Figure: HRTEM image  $Cr_3Ni_5Si_2$   $[001]$ , Titan negative Cs.

# $Cr_3Ni_5Si_2$ observed in $[001]$ projection

Imaging a thicker crystal or changing defocus modify (in general) the HRTEM images (where are the atomic columns?).



Figure: HRTEM image  $Cr_3Ni_5Si_2$   $[001]$ , thickness 10 nm, defocus -8.2 nm.

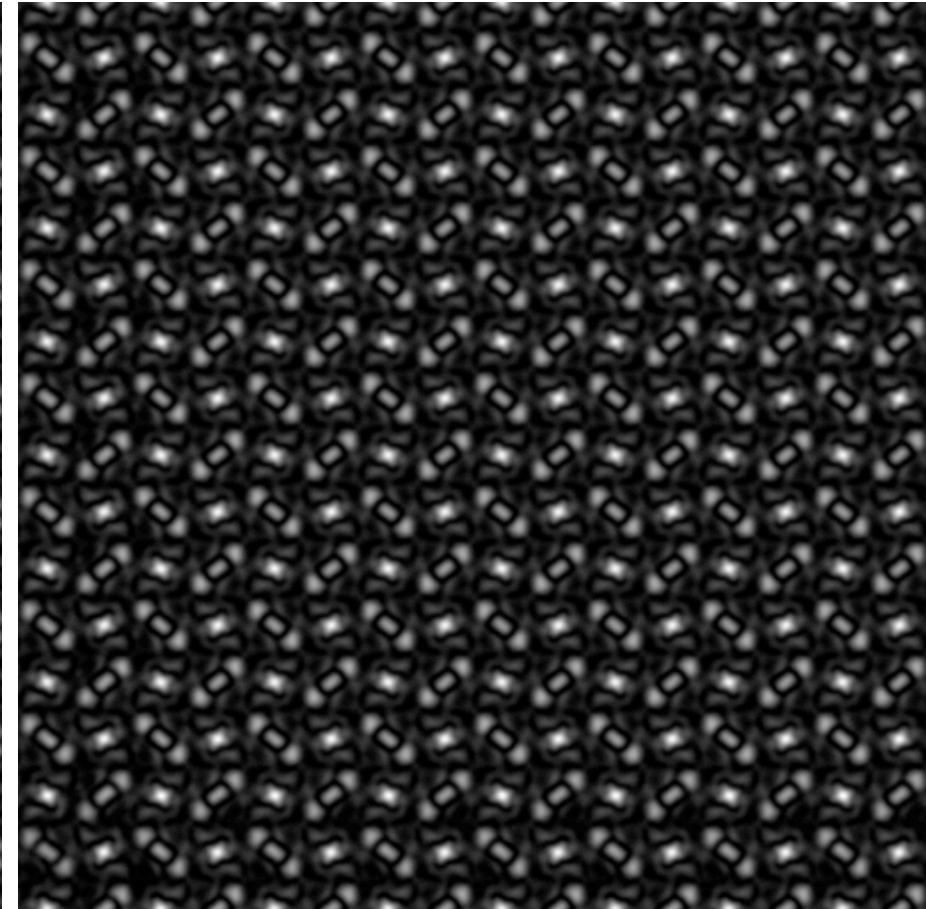


Figure: HRTEM image  $Cr_3Ni_5Si_2$   $[001]$ , thickness 10 nm, defocus 8.2 nm.

# $Cr_3Ni_5Si_2$ observed in [001] projection

Imaging a thicker crystal or changing defocus modify (in general) the HRTEM images (where are the atomic columns?).



Figure: HRTEM image  $Cr_3Ni_5Si_2$  [001], thickness 10 nm, defocus -8.2 nm.

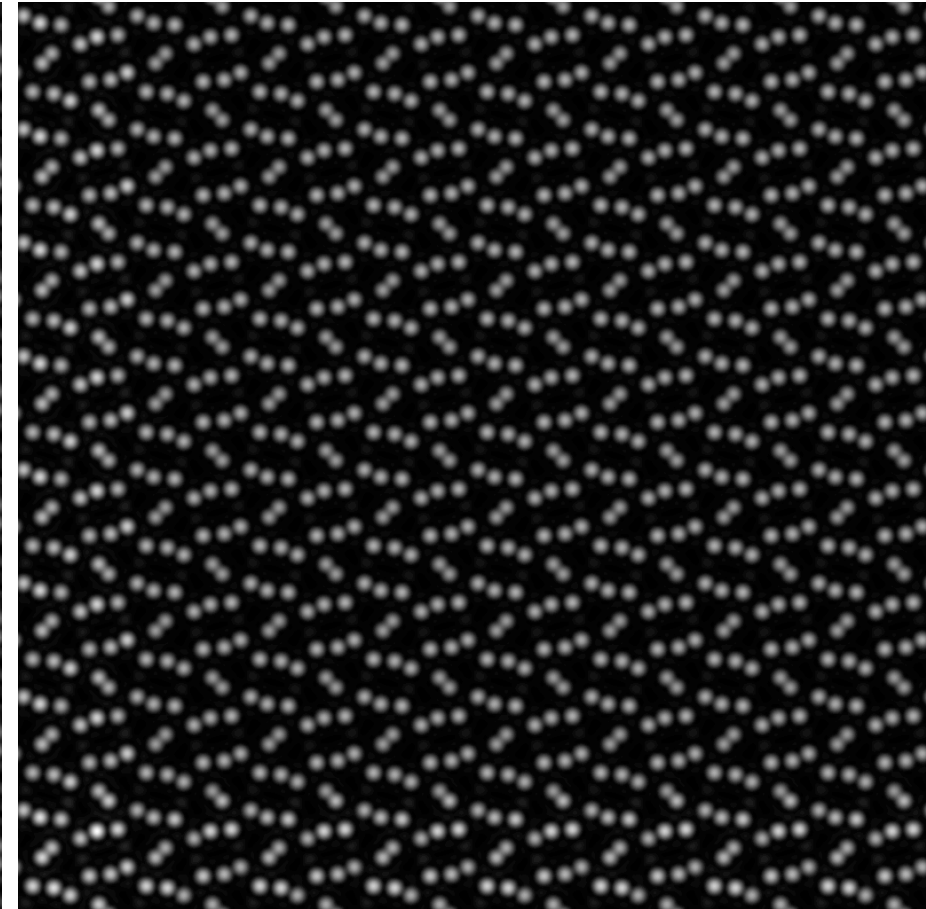


Figure: HAADF image  $Cr_3Ni_5Si_2$  [001], thickness 10 nm.

# $Cr_3Ni_5Si_2$ observed in $[001]$ projection

Imaging a thicker crystal or changing defocus modify (in general) the HRTEM images (where are the atomic columns?).

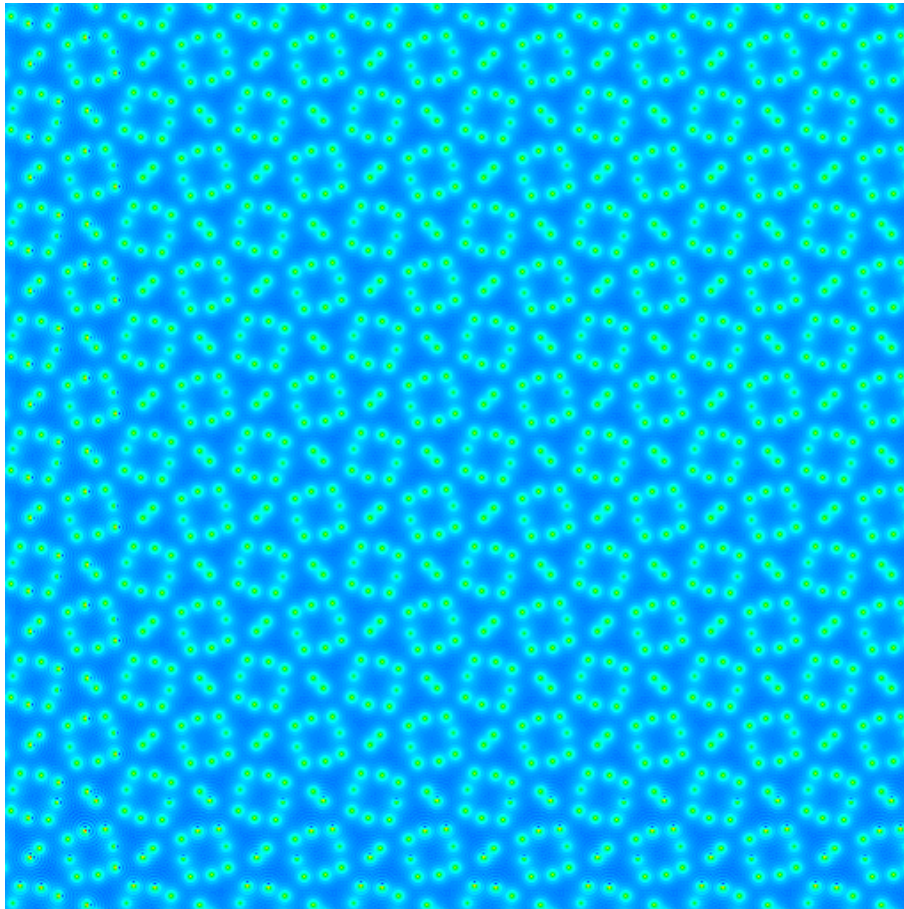


Figure: Projected potential  $Cr_3Ni_5Si_2$   $[001]$ .

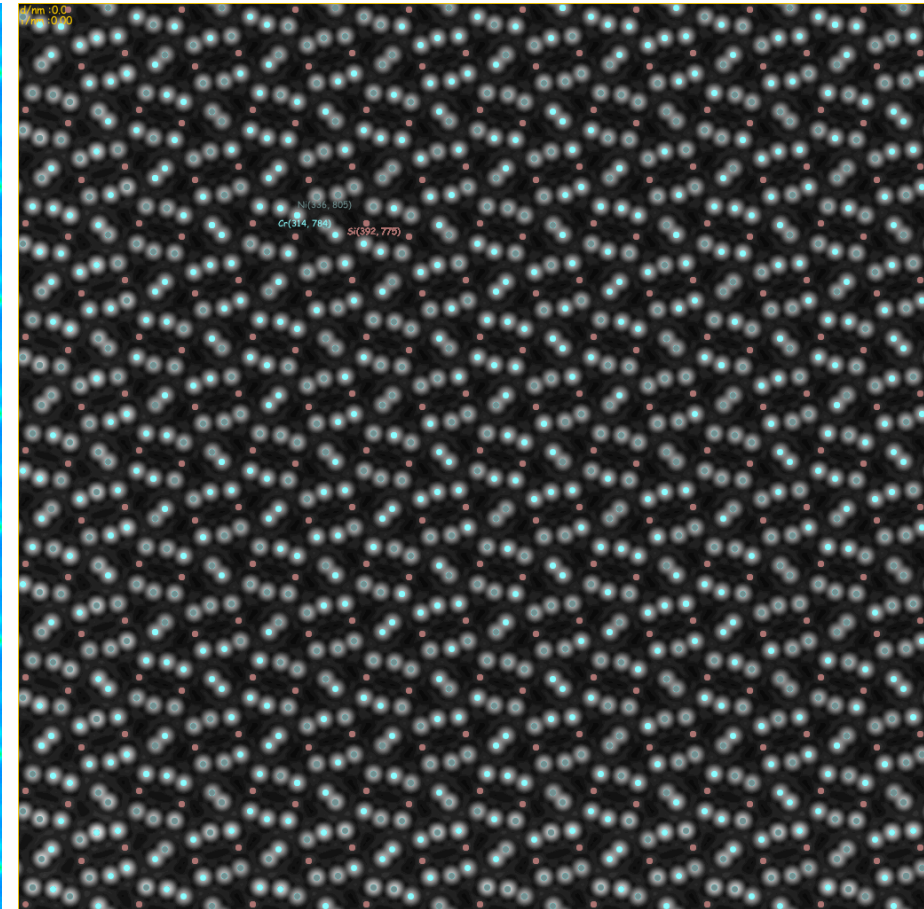


Figure: HAADF image  $Cr_3Ni_5Si_2$   $[001]$ , thickness 10 nm.

# How to do HRTEM or HAADF image simulation?

We need models, (good) approximations and methods.

## 1. Models

### 1.1 Crystal

- ▶ Lattice parameters.
- ▶ Symmetries (space-group, regular point system).
- ▶ Atoms position.
- ▶ Orientation, ( $[uvw]$  zone axis indices,  $(hkl)$  Laue circle center indices with  $u h + v k + w l = 0$  ).
- ▶ Shape (thickness, defect, ...).

### 1.2 Microscope

- ▶ Source coherence (i.e. size, energy spread).
- ▶ Acceleration voltage.
- ▶ Objective lens properties ( $C_s$ , spherical aberration coefficient,  $C_c$ , chromatic aberration coefficient, ...).

### 1.3 Detector: Modulation Transfer Function.

## 2. Approximations

### 2.1 Elastic scattering (under small angle scattering approximation, i.e. acc. voltage $\geq 50$ kV):

- ▶ Kinematical: single scattering.
- ▶ Dynamical: multiple scattering.

### 2.2 Inelastic scattering:

- ▶ Single inelastic scattering.
- ▶ Multiple inelastic scattering.
- ▶ Frozen lattice or frozen phonon.

### 2.3 Abbe imaging theory (transmission cross-coefficients and transfer function).

## 3. Methods

### 3.1 Bloch wave (solid state physics).

### 3.2 Multislice (physical optics).

### 3.3 Howie-Whelan (column approximation).

Models are **not** necessarily crystalline.

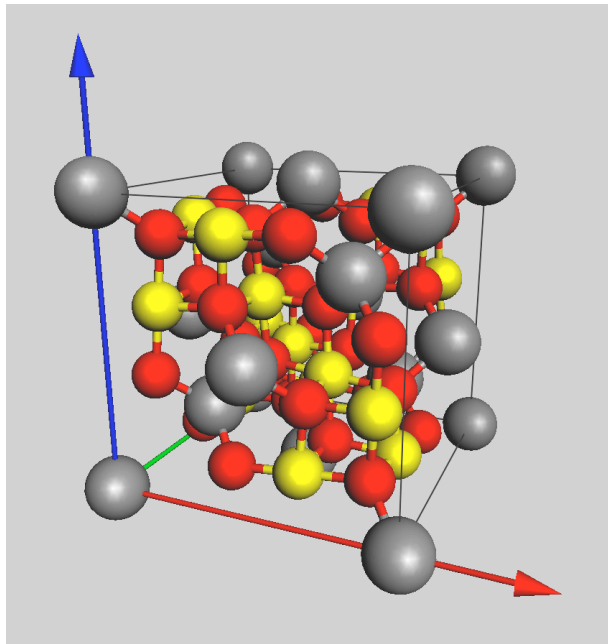


Figure: CoCr<sub>2</sub>O<sub>4</sub> (cubic, F d -3 m, 3 atoms).

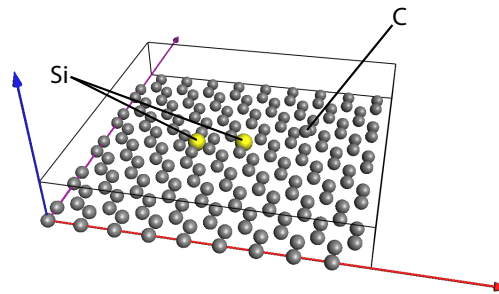


Figure: Graphene sheet with add atoms (448 atoms).

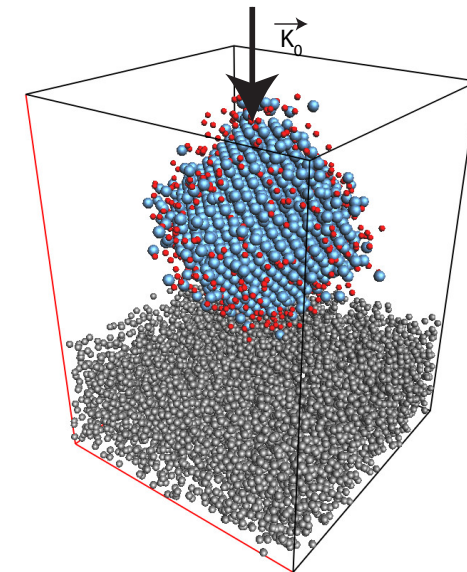
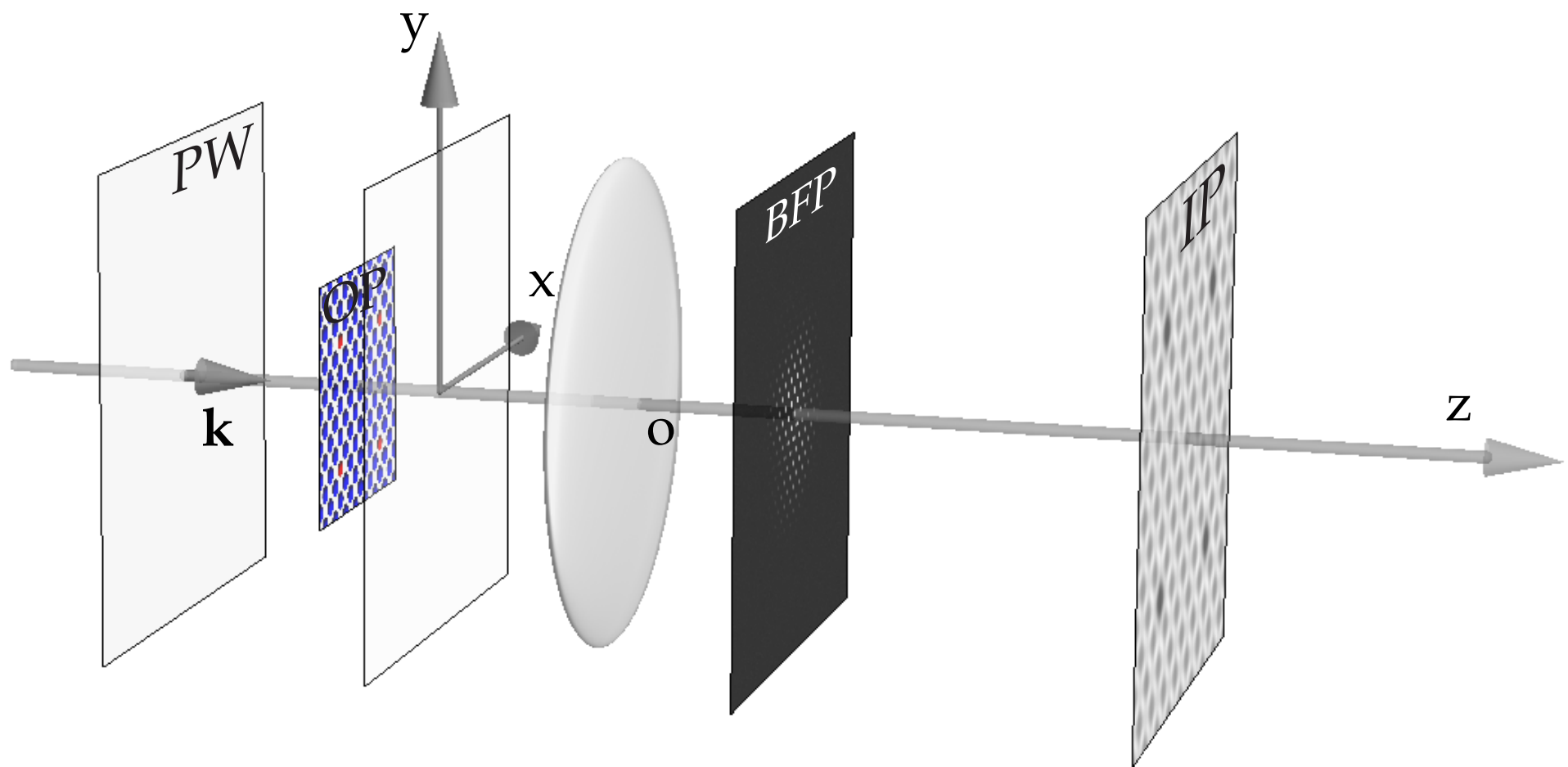


Figure: Pt catalyst (Pt cube octahedron on amorphous carbon film, 10'000 atoms).

A model is a box of parameters  $(a, b, c, \alpha, \beta, \gamma)$  with atoms at  $(x, y, z)$  such that  $0.0 \leq (x, y, z) < 1.0$ . The symmetries (space-group) helps defining the structure, the extinctions, etc.

# Model: the electron microscope



Only the objective lens is modelled and its axial aberrations considered, since it is the first imaging lens and its lateral magnification  $G_l$  is very large (HRTEM). Lateral magnification corresponds to an angular compression  $G_a = \frac{1}{G_l}$  ( $G_l G_a = 1$ ).

# Approximations: scattering

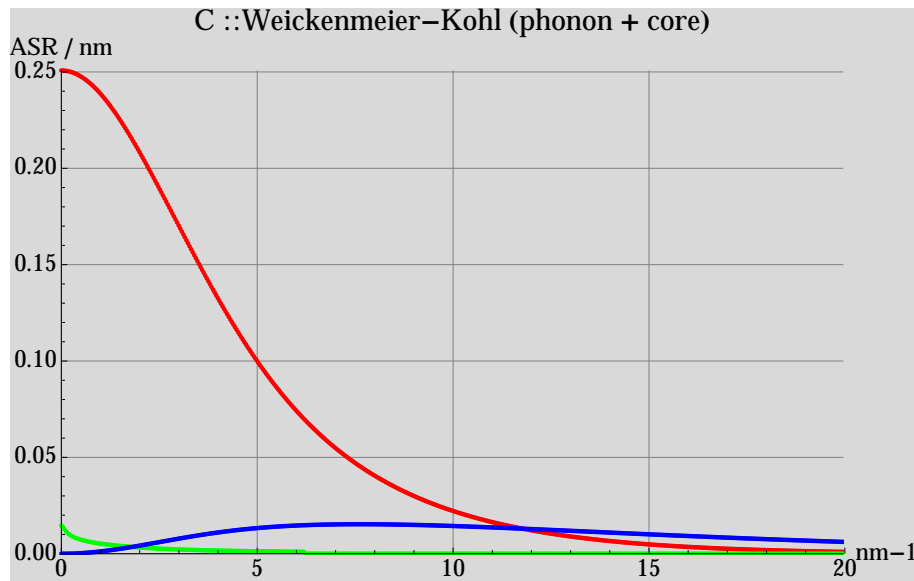


Figure: Atomic Scattering Amplitude (carbone), red: elastic, blue: TDS.

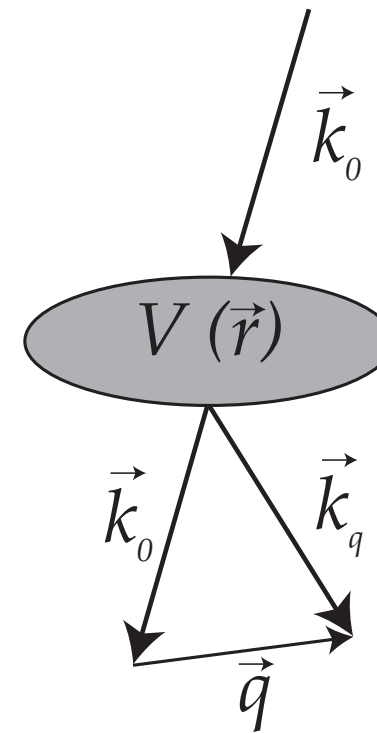


Figure: Electrons interact with the crystal potential  $V(\vec{r})$ .

Scattering:

$$\vec{k}_q = \vec{k}_o + \vec{q}$$

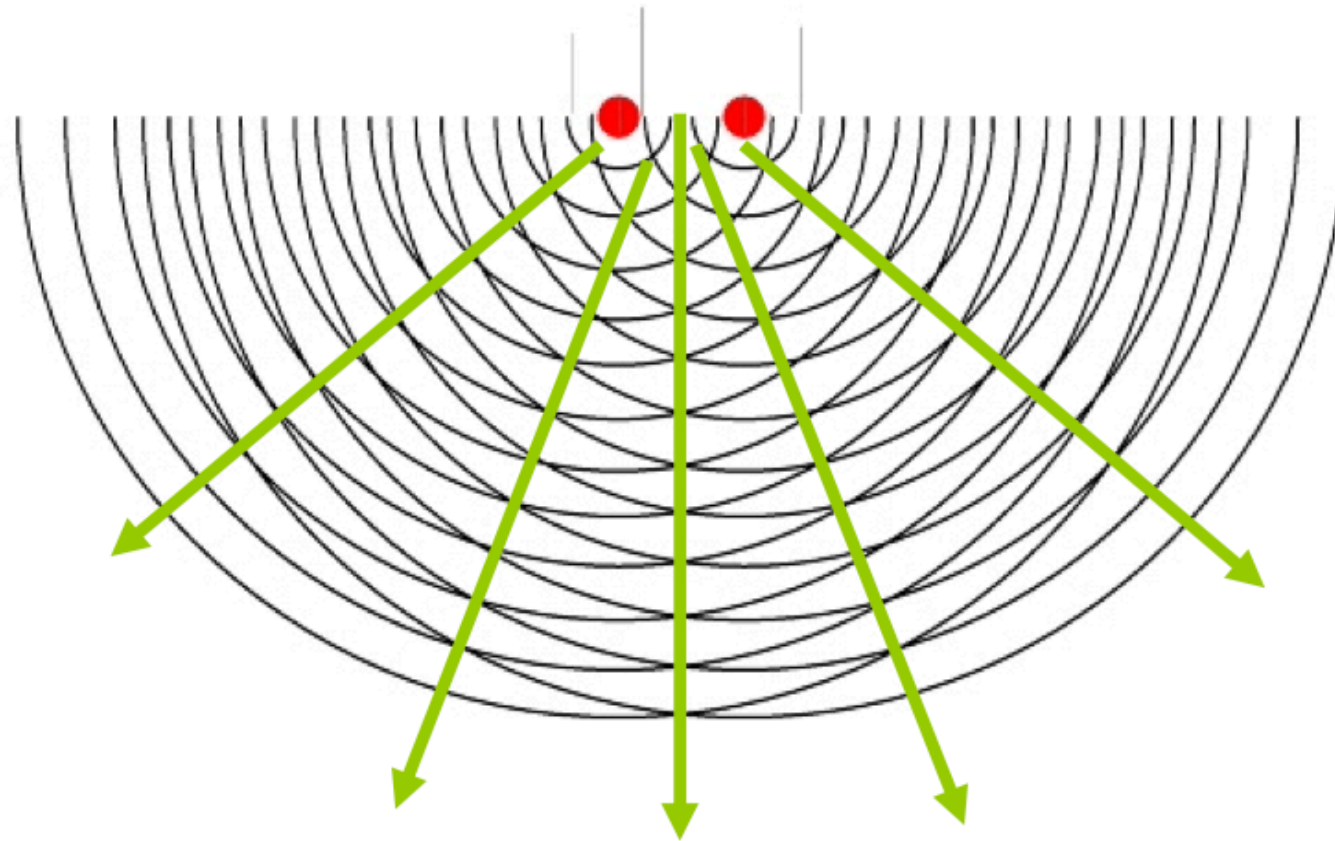
Elastic scattering:

$$||\vec{k}_q|| = ||\vec{k}_o||$$



# Diffraction under kinematical approximation: single scattering by $10^n$ atoms

**Diffraction = scattering by many scattering centres (atoms) and interference of spherical waves emitted by the centres.**



The larger the number of scattering centres the smaller the angular spread of the diffracted beams.

# Structure factors: scattering strength

The structure factor gives the scattering *strength* of any (h,k,l) plane.

$$F_{hkl} = \sum_{i=\text{atomes}} f_i(s_{hkl}) e^{(2\pi i(hx_i + ky_i + lz_i))}$$

where:

1.  $f_i(s_{hkl})$  is the atomic scattering amplitude.
2.  $(x_i, y_i, z_i)$  are the fractional coordinates of atom  $i$  ( $0 \leq x_i < 1$ ).
3.  $s_{hkl} = \frac{\sin(\theta_B)}{\lambda} = \frac{1}{2d_{hkl}}$ .

To plot diffraction patterns under the kinematical approximation one needs to calculate structure factors and reciprocal space geometry only.

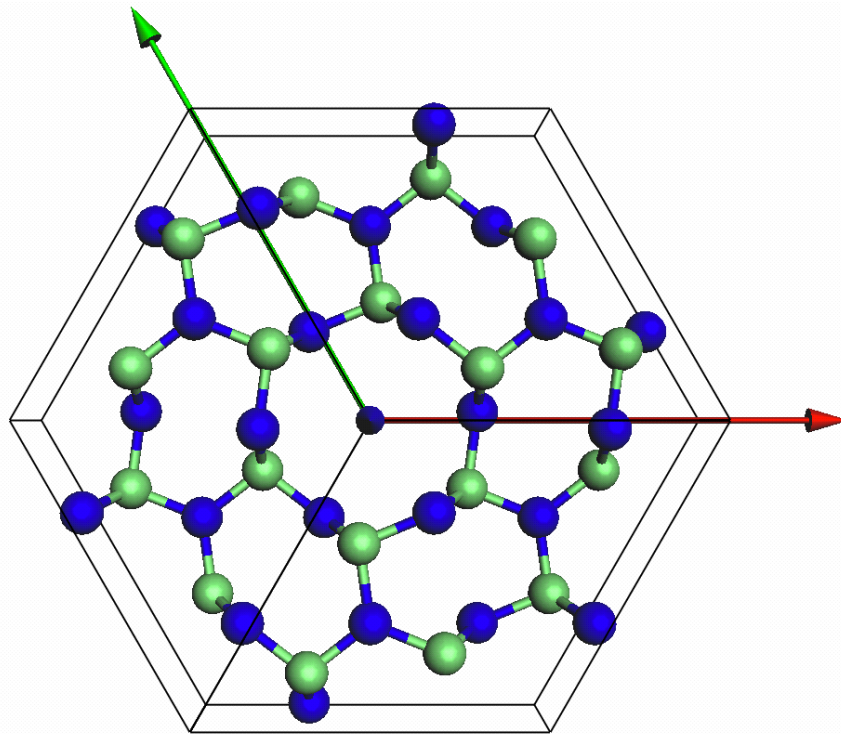


Figure: Model ( $Ge_3N_4$ ).

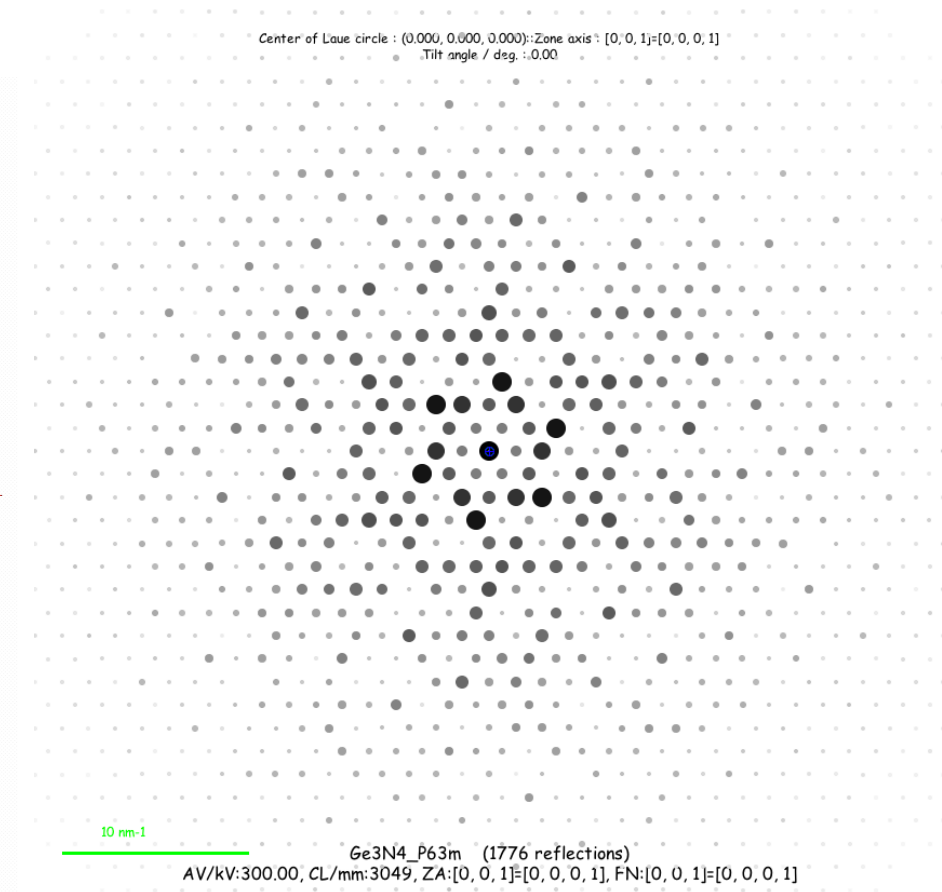


Figure: Kinematical diffraction  $Ge_3N_4$ , [001].

# Dynamical scattering: multiple scattering

Since the electron-matter interaction is very strong ( $10^4$  stronger than that of X-Ray), electrons can be scattered several times. The general framework to describe dynamical scattering is provided by the **Time dependent Schrödinger equation** (electron spin is neglected).

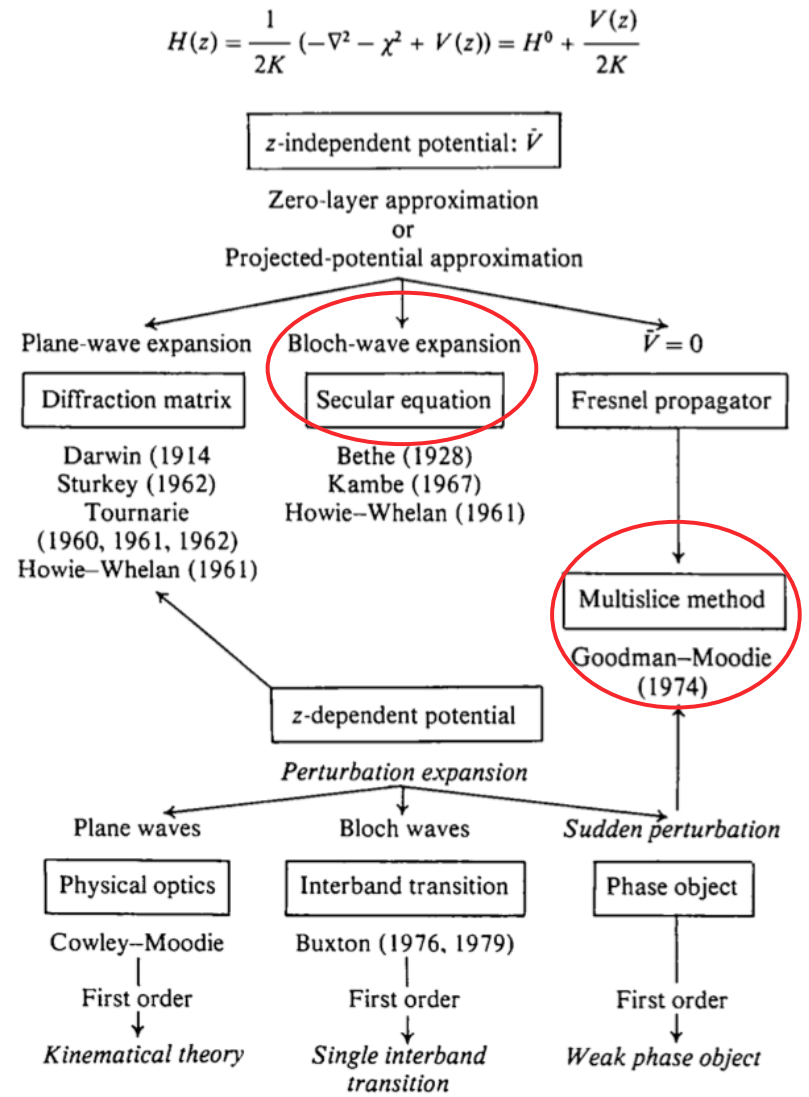
$$i\hbar \frac{\partial}{\partial t} \Psi = (-\Delta + V) \Psi$$

With a few definitions and approximations:

- ▶  $k_0 = \frac{1}{\hbar} \left( 2m_0 E + \frac{E^2}{c^2} \right)^{1/2}$  (incident electron wavelength  $\lambda = \frac{1}{k_0}$ ).
- ▶  $\vec{k}_0 = \vec{k} + \vec{\chi}$  ( $\chi$  : projection of  $k_0$  on Oxy plane).
- ▶  $V = \frac{2}{\hbar^2} \left( m_0 + \frac{E}{c^2} \right) V(\vec{r})$  (relativistic correction).
- ▶ Writing  $\Psi(\vec{r}) = \psi(\vec{\rho}, z) e^{iKz}$  (with  $\vec{\rho} = (x, y)$ ).
- ▶ Stationary flux of electron ( $\Psi \rightarrow$  **time independent**).
- ▶  $||\vec{k}_q|| = ||\vec{k}_o||$  (**elastic scattering**).
- ▶ Small angle scattering  $\frac{\partial^2}{\partial z^2} \psi(\vec{\rho}, z) = 0$  (**electron backscattering is neglected**).

$$i\hbar \frac{\partial}{\partial z} \psi = (-\Delta_{x,y} - \chi^2 + V) \psi$$

# Quantum-mechanical perturbation theory $\rightarrow U(z, 0)$



A must read paper <sup>1</sup>.

<sup>1</sup>D. Gratias and R. Portier, Acta Cryst. **A39** (1983), 576.

# Dynamical scattering: two approximations

All approximations are numerically equivalent, but perform best in particular cases.

We will consider only 2 approximations:

- ▶ The multislice approximation<sup>2</sup>.
- ▶ The Bloch-wave method<sup>3</sup>.

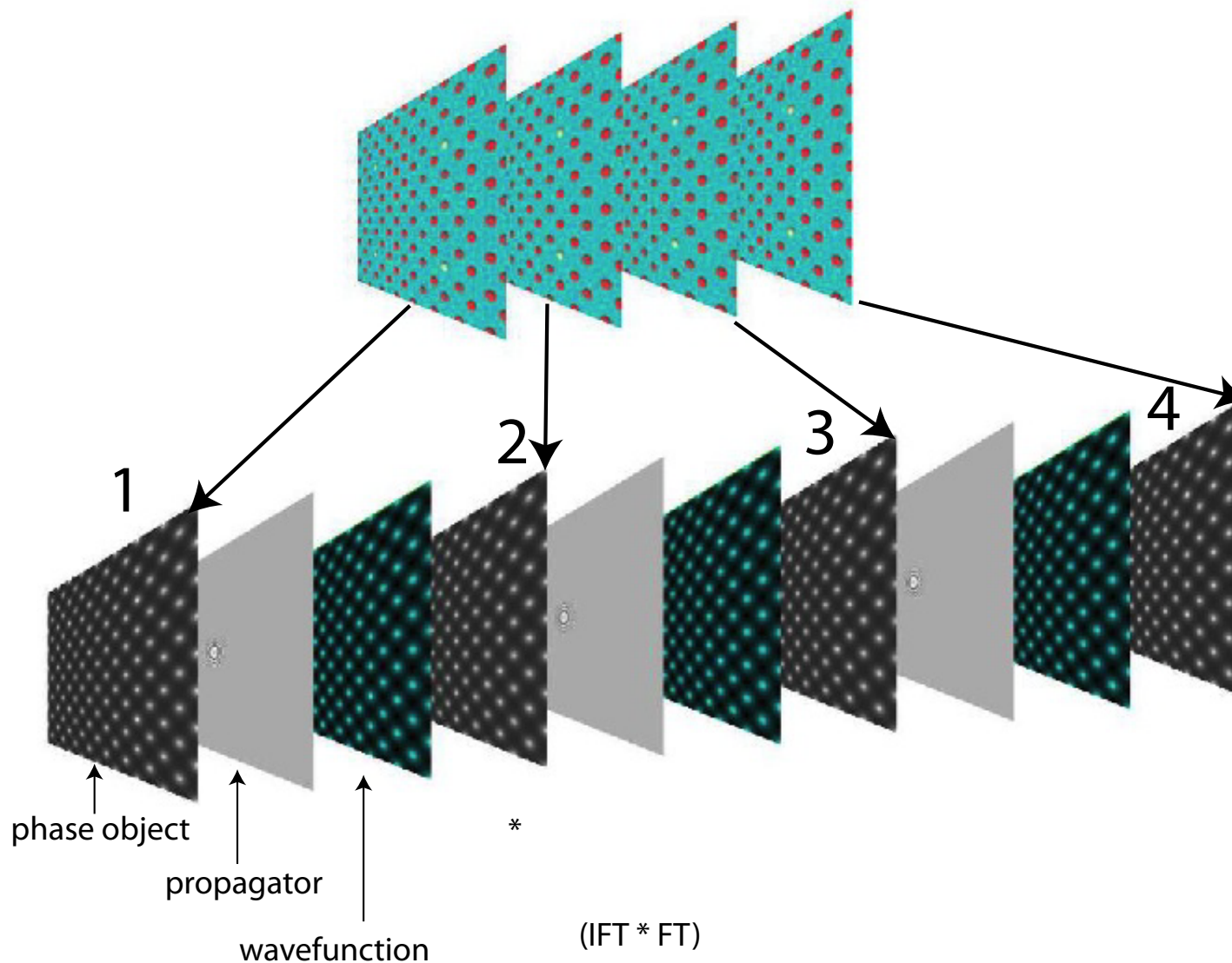
The multislice method performs best when simulating crystalline or amorphous solids of large unit cell or containing defects while the Bloch-wave method is adapted to the calculation of crystalline solids of small unit cell and in any  $[uvw]$  orientation. The Bloch-wave method has also several advantages (speed, ease of use) for simulating CBED, LACBED or PED patterns and for polarity and chirality determination.

---

<sup>2</sup>J. Cowley and A.F. Moodie, Proc. Phys. Soc. B70 (1957) 486, 497 and 505.

<sup>3</sup>H. A. Bethe, Ann. Phys. 87 (1928), 55.

# Dynamical scattering calculations: multislice method



A very popular (and powerful) method for performing dynamical calculation has been proposed by J. M. Cowley and A.F. Moodie. It makes use of several principles of Optical Physics.

# Bloch wave method: z-independent potential

When the scattering potential is periodic, the eigenstates  $|j\rangle$  of the propagating electrons are Bloch waves. The hamiltonian of the system is projected on the eigenstates  $|j\rangle$  with eigenvalues  $\gamma_j$  ("anpassung" parameter).

$$\hat{H} = \sum_j \gamma_j |j\rangle \langle j|$$

The evolution operator is then given by (since  $V = V(\vec{\rho})$ ):

$$\hat{U}(z, 0) = e^{-i\hat{H}z} = \sum_j e^{-i\gamma_j z} |j\rangle \langle j|$$

The wave-function at z developed on plane waves basis  $|q\rangle$ :

$$\Psi(z) = \sum_q \phi_q(z) |q\rangle$$

$$\phi_q(z) = \langle q | \hat{U}(z, 0) | 0 \rangle = \sum_j e^{-i\gamma_j z} \langle q | j \rangle \langle j | 0 \rangle$$

$$c_0^{*j} = \langle j | 0 \rangle \quad \text{and} \quad c_q^j = \langle q | j \rangle$$

where in usual notation  $c_0^{*j}$  and  $c_q^j$  are the Bloch-wave excitations (component of the initial state  $|0\rangle$  on  $|j\rangle$ ) and coefficients (component of reflection  $|q\rangle$  on  $|j\rangle$ ) respectively.



# Bloch wave coefficients $c_0^{*j}$ and $c_q^j$

The Bloch wave coefficients  $c_0^{*j}$  and  $c_q^j$  are determined from:

$$\begin{aligned}\hat{H}|j\rangle &= \gamma_j|j\rangle \Rightarrow \langle q|\hat{H}|j\rangle = \gamma_j \langle q|j\rangle \\ \langle q|\frac{1}{2k_z}(-\hat{\Delta} - \chi^2 + \bar{V})|j\rangle &= \gamma_j \langle q|j\rangle \\ \frac{q^2 - \chi^2}{2k_z} \langle q|j\rangle + \sum_{q'} \langle q|\frac{\bar{V}}{2k_z}|q'\rangle \langle q'|j\rangle &= \gamma_j \langle q|j\rangle \\ \frac{q^2 - \chi^2}{2k_z} c_q^j + \frac{V_{q'-q}}{2k_z} c_{q'}^j &= \gamma_j c_q^j\end{aligned}$$

It is transformed in an homogenous system (in matrix form) on the (complete) *basis*  $\{g\}$  formed by the plane waves:

$$\left[ \left[ \frac{g^2 - \chi^2}{2k_z} - \lambda \hat{I} + \frac{\bar{V}_{h-g}}{2k_z} \right] \right] [c] = 0$$

The eigenvalues  $\gamma_j$  and eigenvectors  $[c]$  are determined for a limited set of plane wave  $|g_i\rangle$ . In practice, the set dimension is increased until the eigenvalues converge. The Bloch waves are finally given by:

$$|j^{(n)}\rangle = \sum_i c_i^n |g_i\rangle$$

The Bloch waves (eigenstates of different energy) propagate independently in the crystal.

# Example: ZnTe [110]

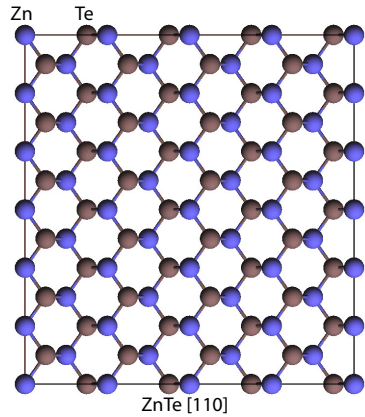


Figure: ZnTe [110].

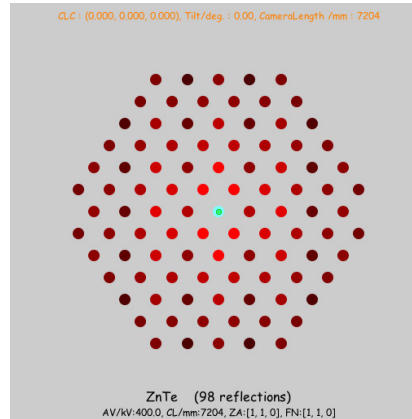


Figure: Reflections (1 + 49),  $|\chi| \geq 0$ .

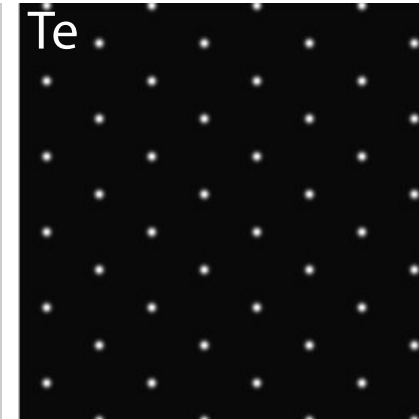


Figure: Bloch-wave 1 (Te 1s).

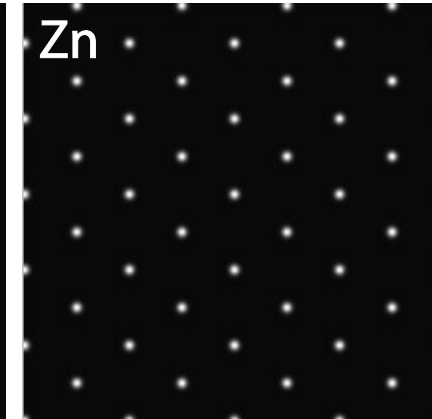


Figure: Bloch-wave 2 (Zn 1s).

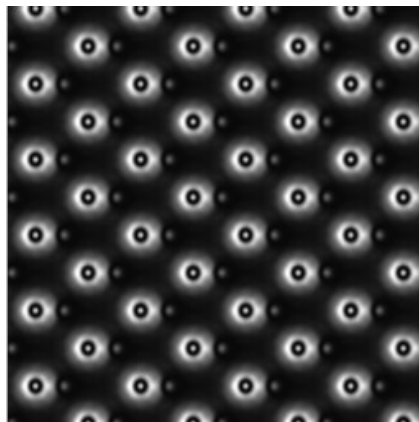


Figure: Bloch-wave 5 (Te-Zn).

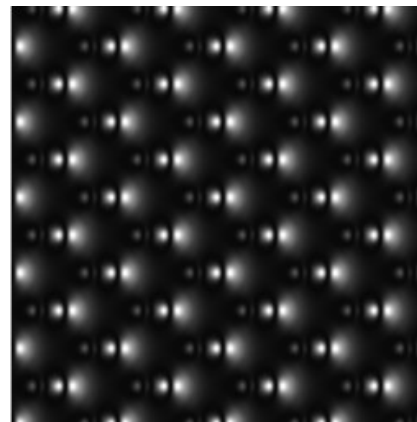


Figure: Bloch-wave 7 (Te-Zn).

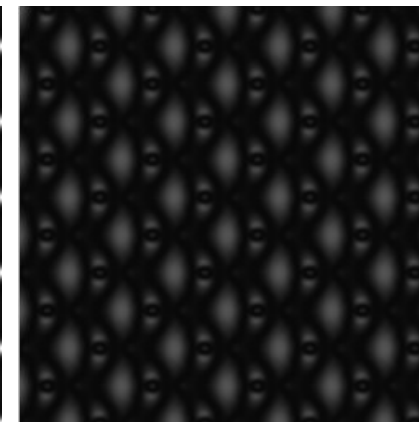


Figure: Bloch-wave 8 (Te-Zn).

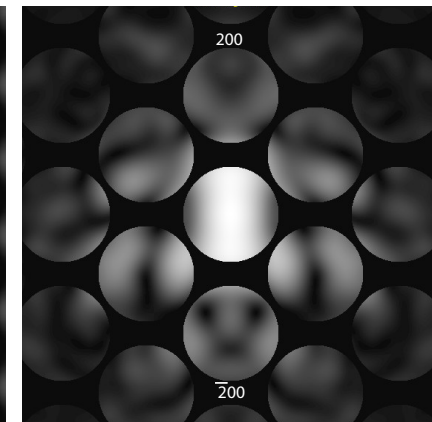


Figure: CBED (ZnTe polarity).

Bloch-wave approach excellent for determining polarity<sup>4</sup>

<sup>4</sup><file:///localhost/Applications/jemsMacOSX/html/ZnO/ZnO.html>

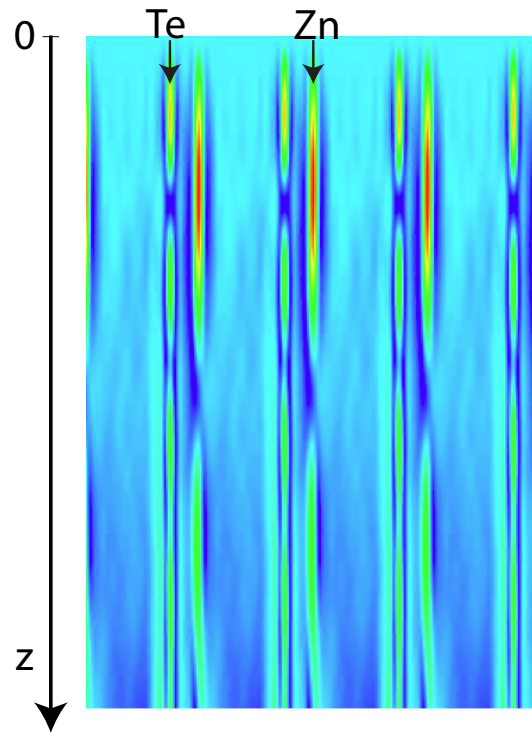


Figure: ZnTe [110] wave-function.

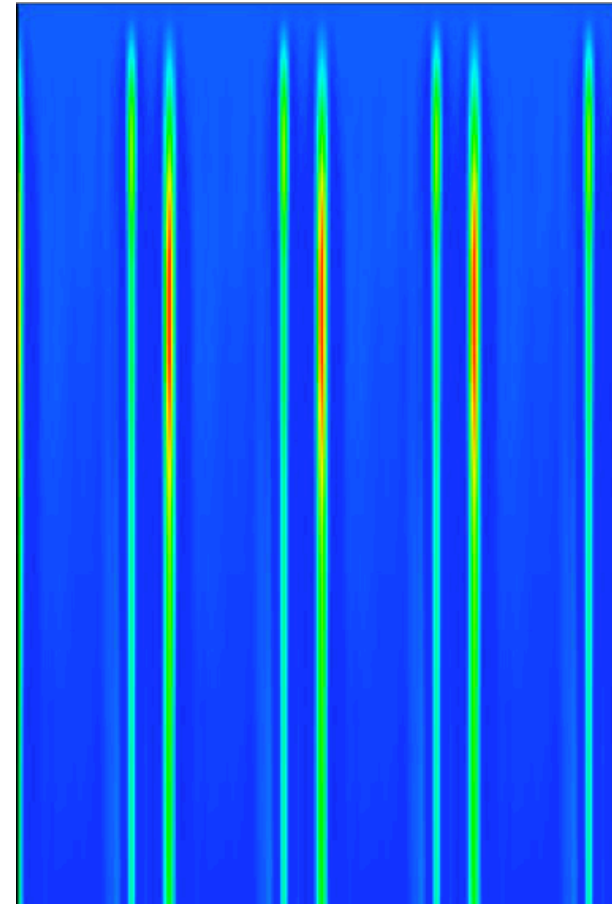


Figure: ZnTe [110] integrated intensity.

Channeling explains several features of HRTEM<sup>5 6</sup> and STEM<sup>7 8</sup> images.

<sup>5</sup>file://localhost/Applications/jemsMacOSX/html/channeling/wavSide.html

<sup>6</sup>file://localhost/Applications/jemsMacOSX/html/channeling/wavTop.html

<sup>7</sup>file://localhost/Applications/jemsMacOSX/html/channeling/side.html

<sup>8</sup>file://localhost/Applications/jemsMacOSX/html/channeling/top.html

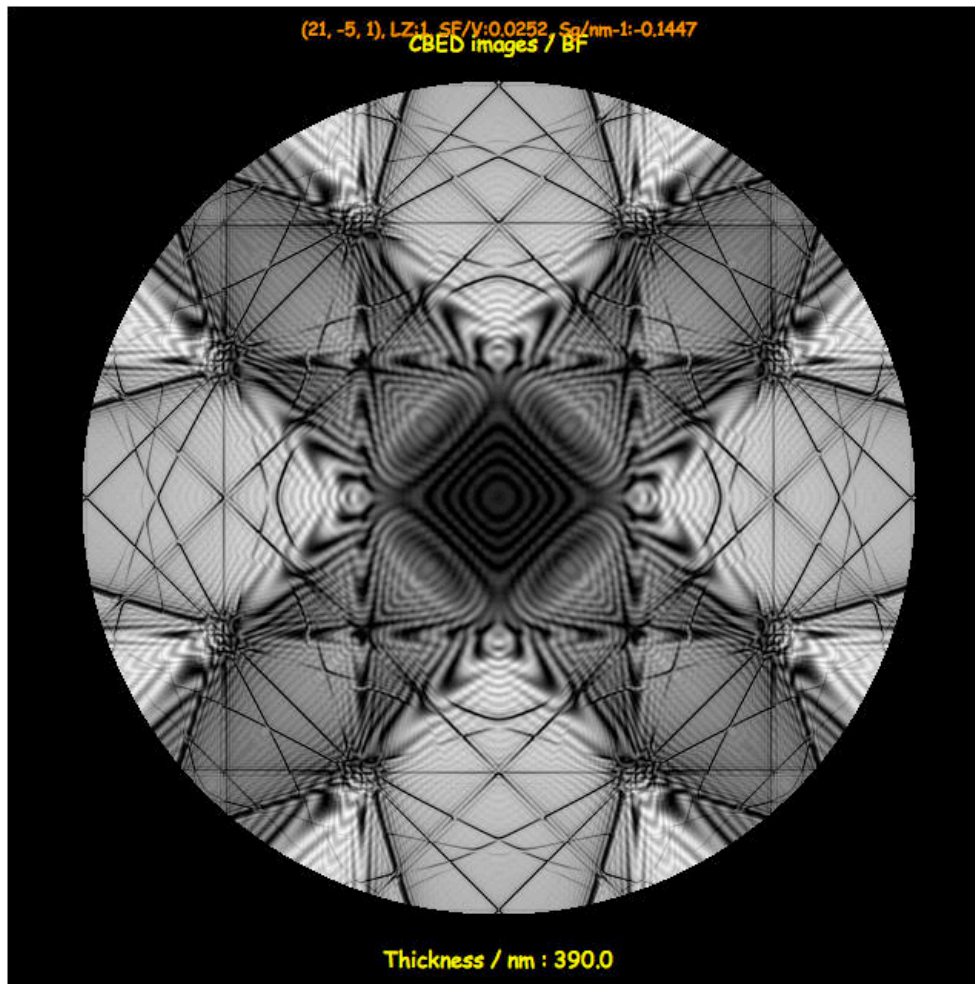


Figure: LACBED Si [001]: simulation.

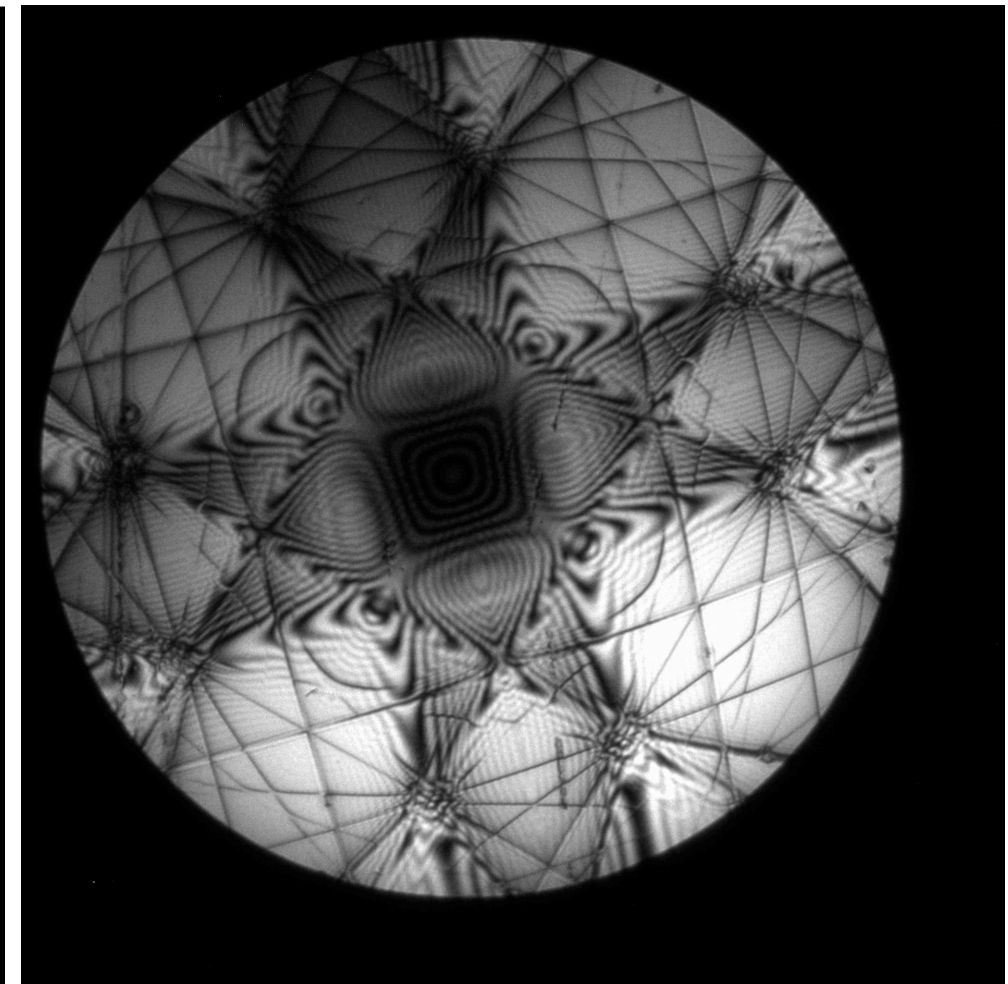
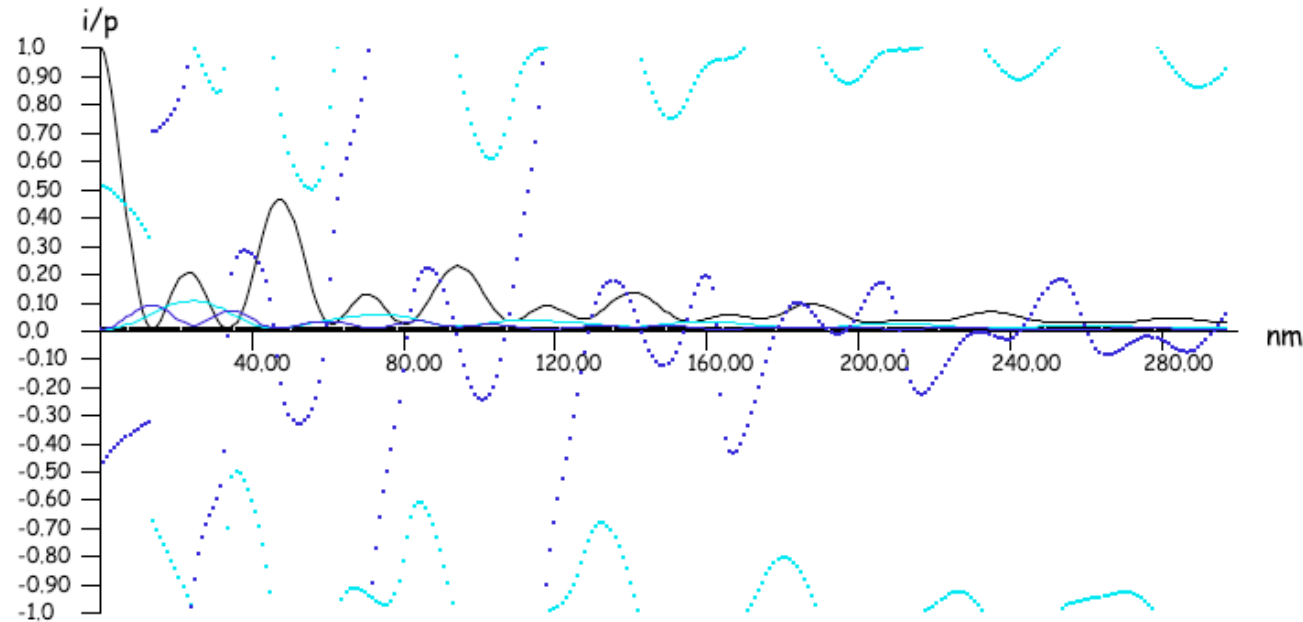


Figure: LACBED Si [001]: experimental (Web site EM centre - Monash university, J. Etheridge).

<sup>9</sup>file://localhost/Applications/jemsMacOSX/html/Si001/Si001.html

# Dynamical scattering: $\text{CoCr}_2\text{O}_4$ [001]

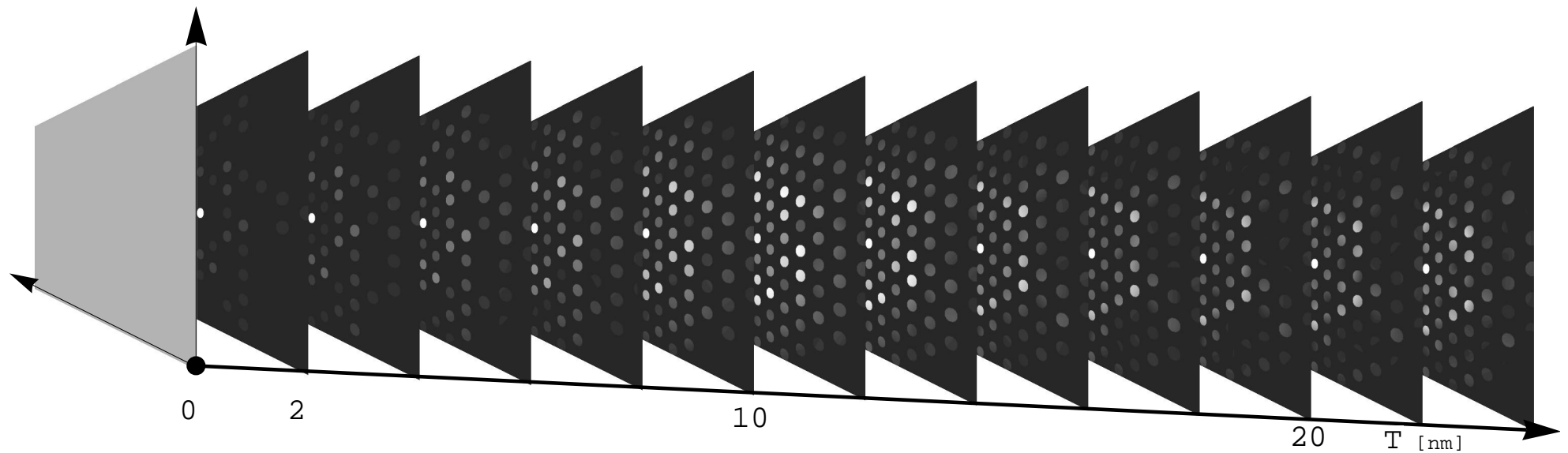
$\text{CoCr}_2\text{O}_4::(4, 0, 0)::[0, 0, 1]::(0.000, 0.000, 0.000)$



0 2 4  
0 2 0  
0 2 0  
0 0 0

**Figure:** Dynamical scattering, i.e. electrons suffer multiple scattering events during their interaction with  $V(\vec{r})$ , makes the amplitude & phase of the transmitted (i.e. unscattered) beam and the reflections (scattered beams) vary widely as a function of specimen thickness.

# Dynamical scattering: thickness series



The extinction distance is related to the Pendellösung period.

# Dynamical scattering: channeling

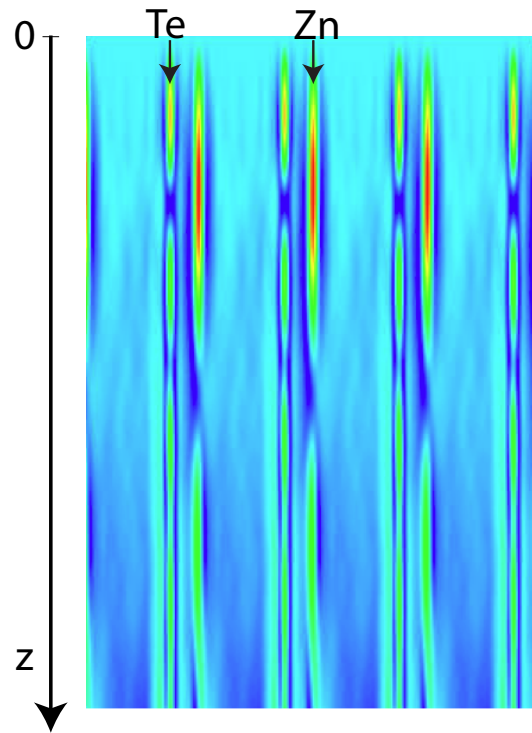


Figure: ZnTe [110] wave-function.

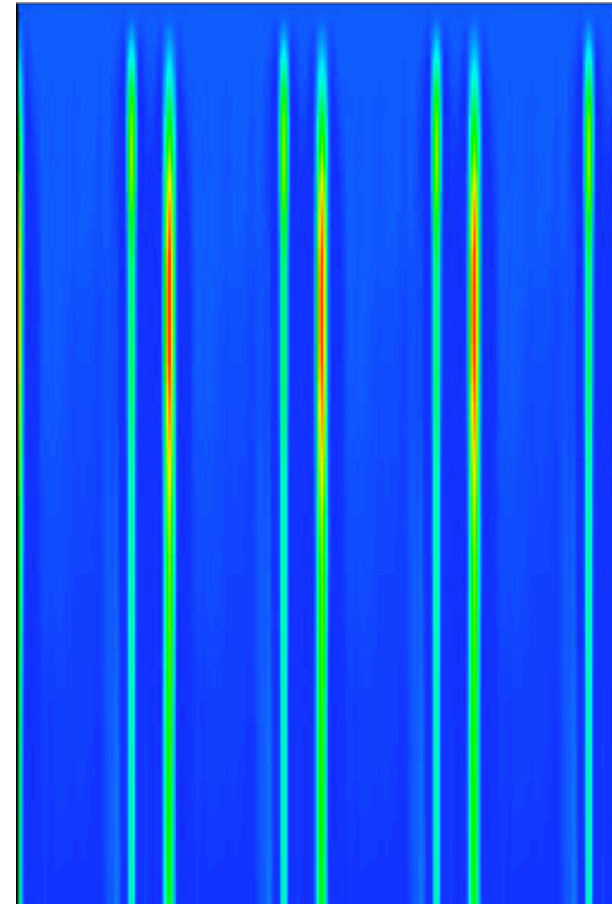


Figure: ZnTe [110] integrated intensity.

Channeling explains several features of HRTEM<sup>10 11</sup> and STEM<sup>12 13</sup> images.

<sup>10</sup>file://localhost/Applications/jemsMacOSX/html/channeling/wavSide.html

<sup>11</sup>file://localhost/Applications/jemsMacOSX/html/channeling/wavTop.html

<sup>12</sup>file://localhost/Applications/jemsMacOSX/html/channeling/side.html

<sup>13</sup>file://localhost/Applications/jemsMacOSX/html/channeling/top.html

## 1. Bad

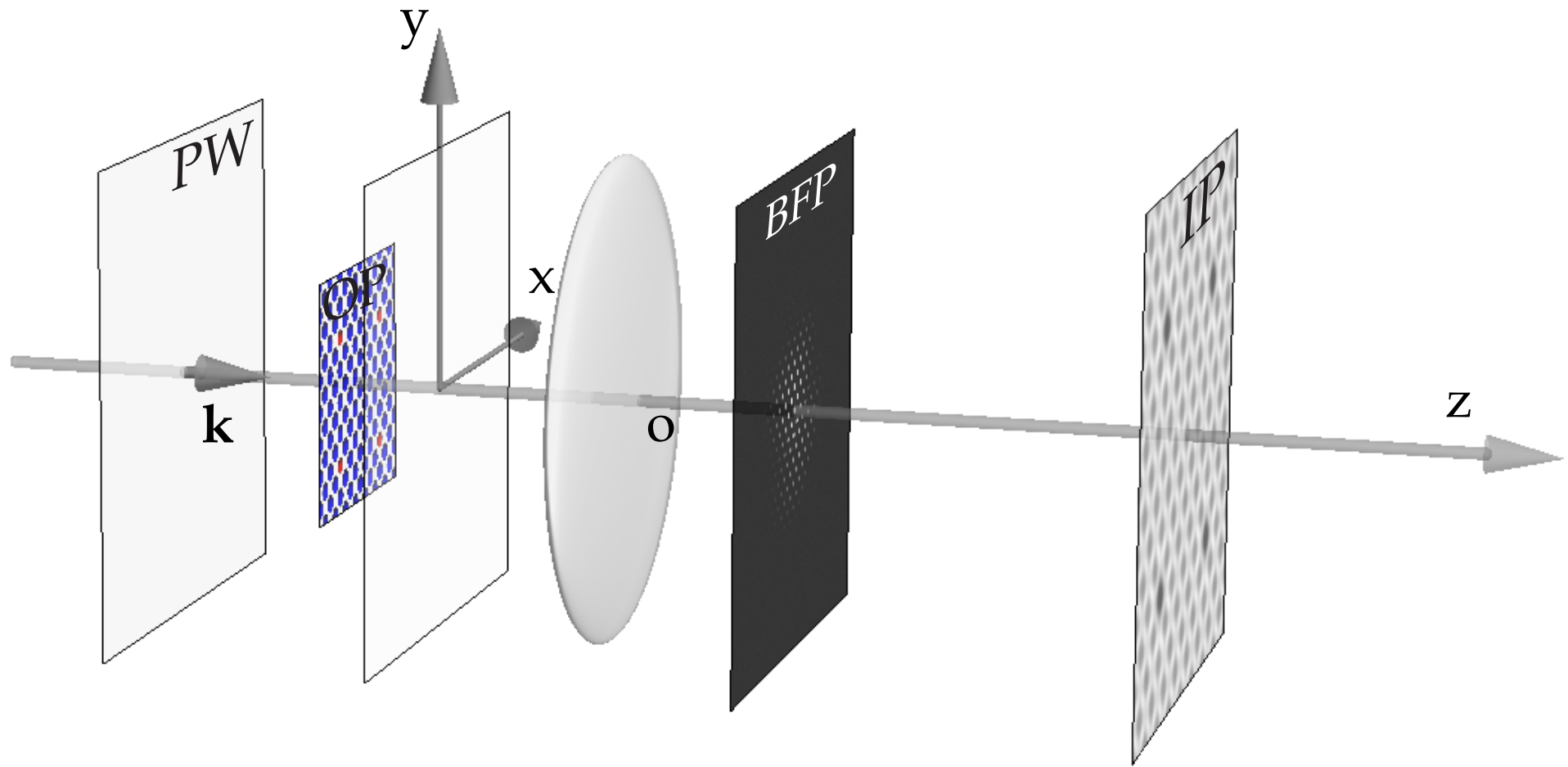
- ▶ Phase relationship between transmitted and diffracted beams depends on thickness → HRTEM lattice fringes or contrast not always on atomic column position.
- ▶ Amplitude of transmitted and diffracted beams depends on thickness → Some HRTEM lattice fringes may be missing or supplementary ones present.

## 2. Good

- ▶ Specimen thickness can be determined precisely ( $\sim 1$  nm or better).
- ▶ Specimen polarity can be determined.
- ▶ Specimen deformation can be determined precisely.



# Model: electron microscope



The electron microscope transfer is modelled by a transfer function  $\tilde{T}(\vec{u})$  that acts only in its Back Focal Plane (BFP). The BFP is the plane where the Fourier transform of the object wave function  $\tilde{\Psi}_o(\vec{u})$  is formed. In the Image Plane, the image intensity is  $\Psi_i(\vec{x}) \Psi_i(\vec{x})^*$  i.e. the modulus square of the image wave function  $\Psi_i(\vec{x})$ .

Transfer of the wave function by the objective lens of the model microscope (**linearity and space invariance**).

**TEM:**

→ **TEM** ( $\tilde{T}(\vec{u})$ ): **T**ransfer **F**unction):

$$\tilde{\Psi}_i(\vec{u}) = \tilde{\Psi}_o(\vec{u}) \tilde{T}(\vec{u})$$

$$\Psi_i(\vec{x}) = \int \tilde{\Psi}_o(\vec{u}) \tilde{T}(\vec{u}) e^{2\pi i \vec{u} \cdot \vec{x}} d\vec{u}$$

**STEM:**

→ **STEM** ( $\widetilde{OTF}(\vec{u}) = \tilde{T}(\vec{u}) \otimes \tilde{T}(-\vec{u})$ ): **O**ptical **T**ransfer **F**unction):

$$I(\vec{x}) = \langle \Psi_i(\vec{x}; t) \Psi_i^*(\vec{x}; t) \rangle$$

$$\Psi_i(\vec{x}; t) = \Psi_o(\vec{x}; t) \otimes T(\vec{x})$$

$$I(\vec{x}) = \langle [\Psi_o(\vec{x}; t) \otimes T(\vec{x})] [\Psi_o^*(\vec{x}; t) \otimes T^*(\vec{x})] \rangle \quad (\otimes \text{ convolution.})$$

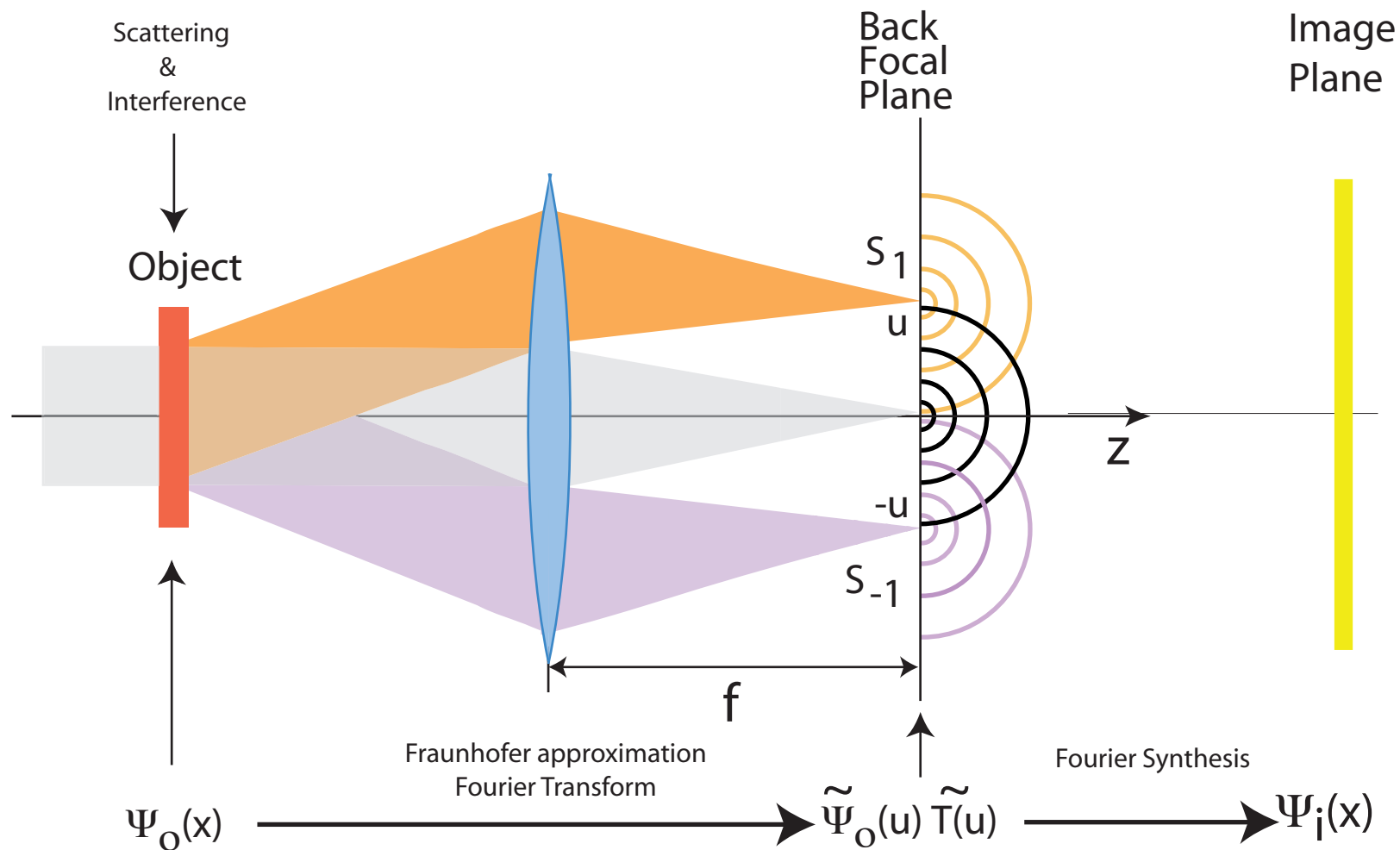
$$I(\vec{x}) = [T(\vec{x}) T^*(\vec{x})] \otimes \langle \Psi_o(\vec{x}; t) \Psi_o^*(\vec{x}; t) \rangle \quad (T(\vec{x}) \text{ is time independent.})$$

$$\langle \Psi_o(\vec{x}; t) \Psi_o^*(\vec{x}; t) \rangle = |\Psi_o(\vec{x})|^2 \quad (\text{complete spatial incoherence})$$

$$I(\vec{x}) = |\Psi_o(\vec{x})|^2 \otimes [T(\vec{x}) T^*(\vec{x})]$$

$$I(\vec{x}) = I_o(\vec{x}) \otimes OTF(\vec{x})$$

# Transfer function: Abbe image formation

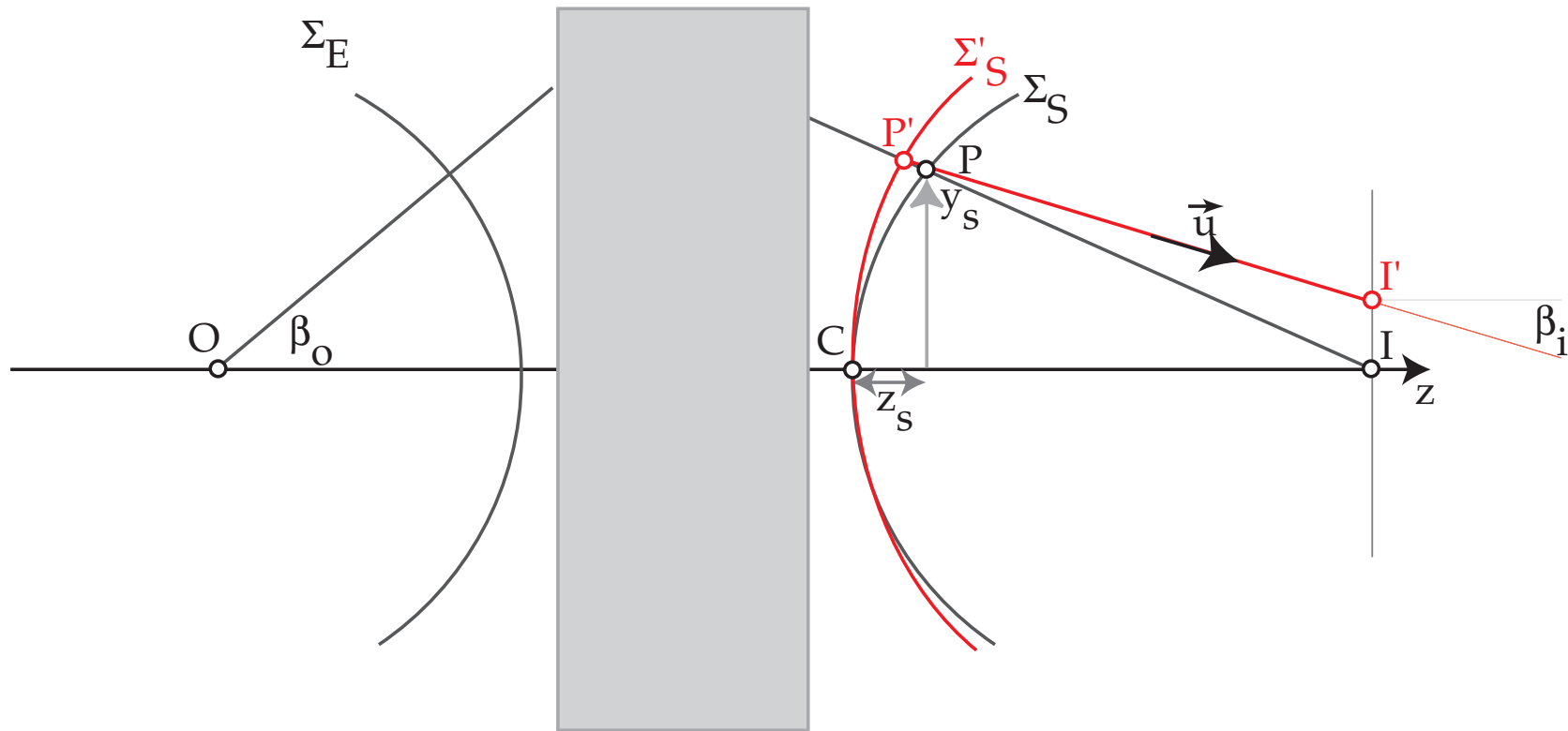


The objective lens changes the phase relationship between the transmitted and diffracted beams. Moreover not all diffracted beams are transmitted, due to its small acceptance angle. High spatial frequencies (i.e. beams diffracted at large angles) are damped due to partial spatial and temporal coherence, electronic noise, mechanical vibrations or drift.

# Difference of OPL: OPD

The OPD measure the deviation of a wavefront from a perfect spherical wavefront (vacuum or homogenous medium).

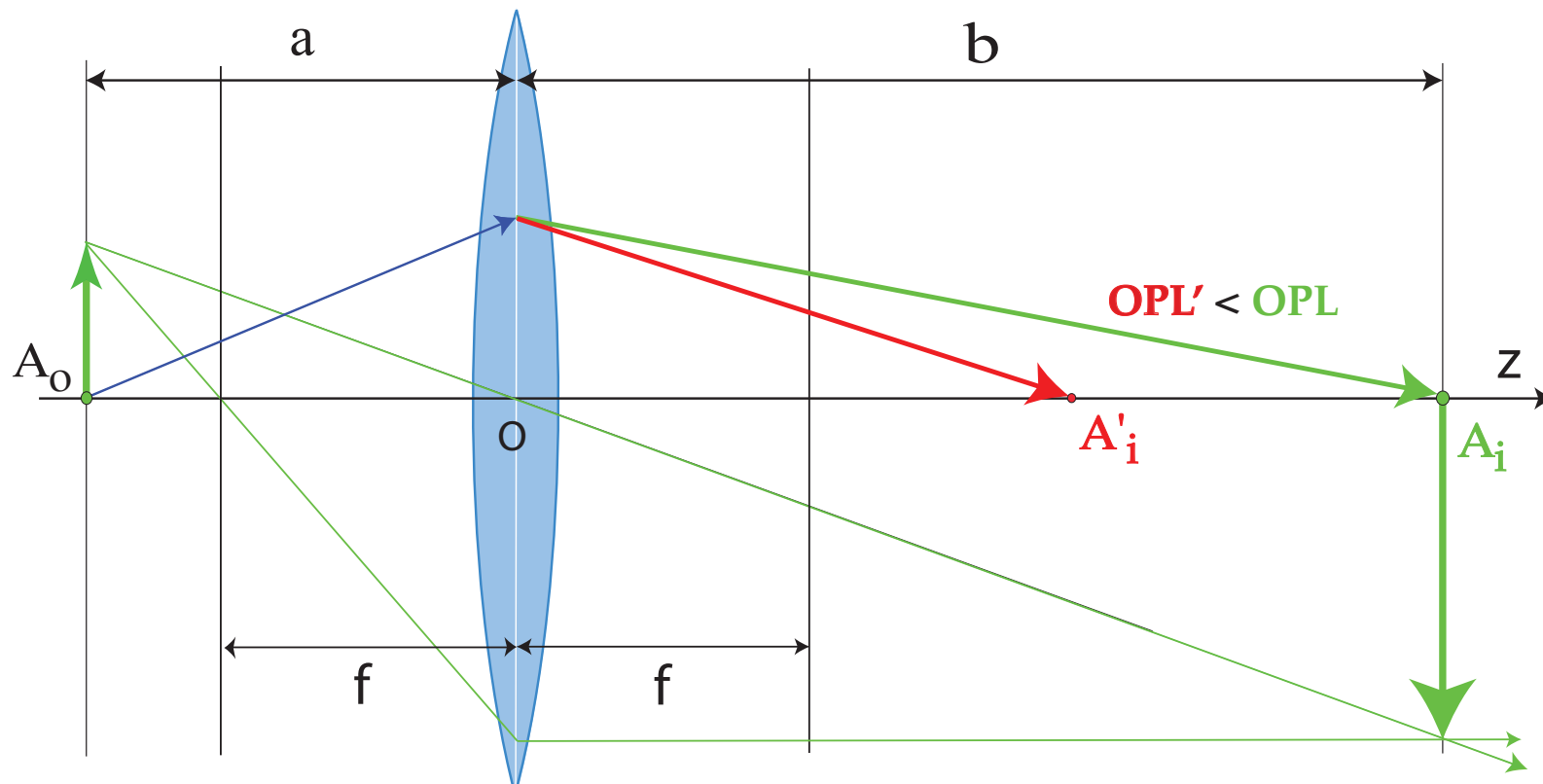
At the exit pupil  $P_S$ , the spherical wavefront converging towards  $I$  defines the reference wavefront.



In the presence of aberrations the wavefront  $\Sigma'_S$  is no more spherical. The **O**ptical **P**ath **D**ifference (distance between the deformed  $\Sigma'_S$  and spherical waveform  $\Sigma_S$ ) introduces the phase shift  $\delta\phi$ :

$$\delta\phi = e^{2\pi i \frac{OPD(x_s, y_s)}{\lambda}}$$

# OPD: spherical aberration

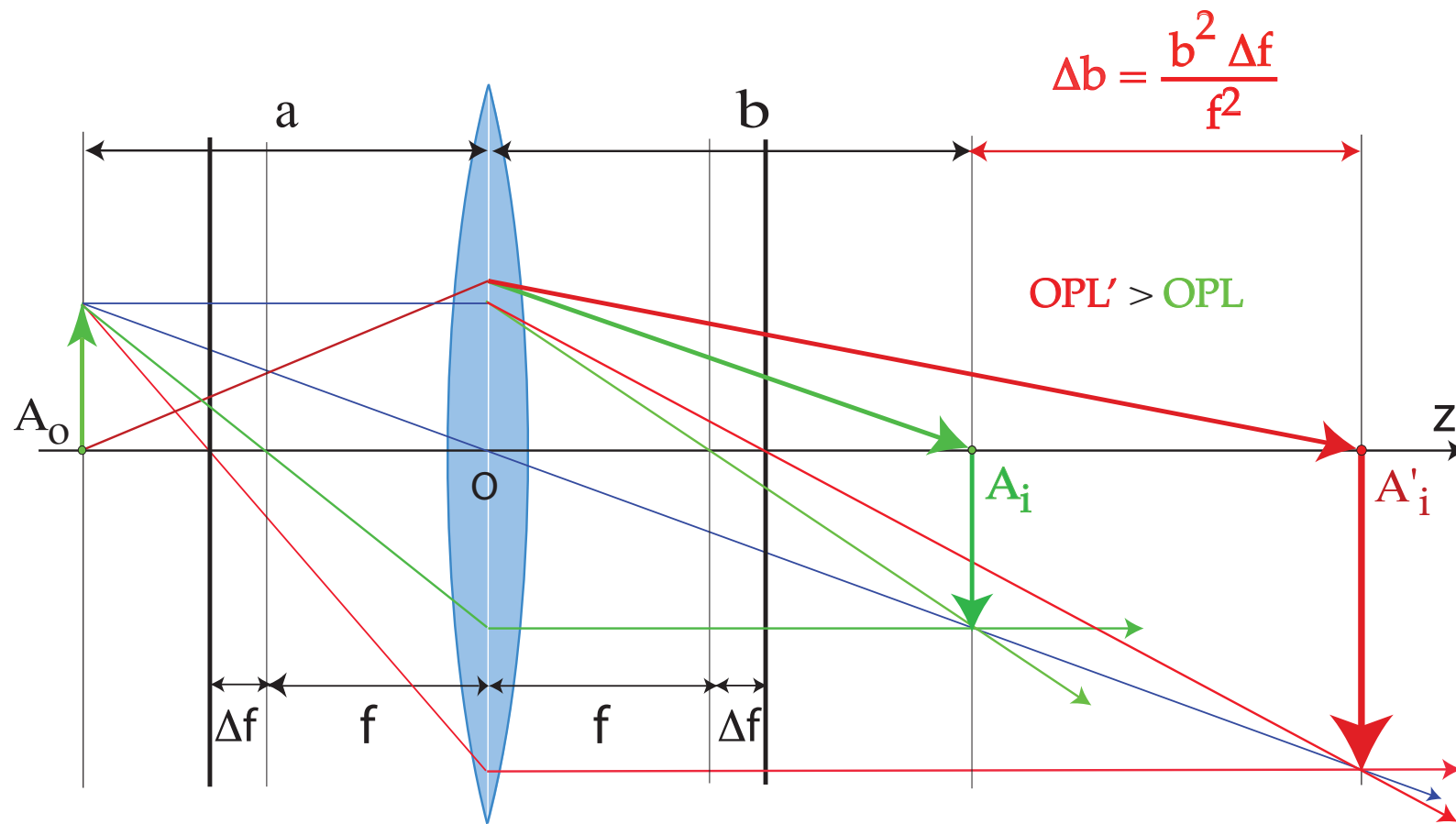


In presence of spherical aberration, the optical path length (OPL') from  $A_o$  to  $A'_i$  is smaller than OPL from  $A_o$  to  $A_i$ . The wavefront at  $A'_i$  is out-of-phase by<sup>14</sup>:

$$e^{-2\pi i \frac{C_s \lambda^3 (\vec{q} \cdot \vec{q})^2}{4}}$$

<sup>14</sup>With our plane wave choice  $e^{+2\pi i \vec{q} \cdot \vec{r}}$ .

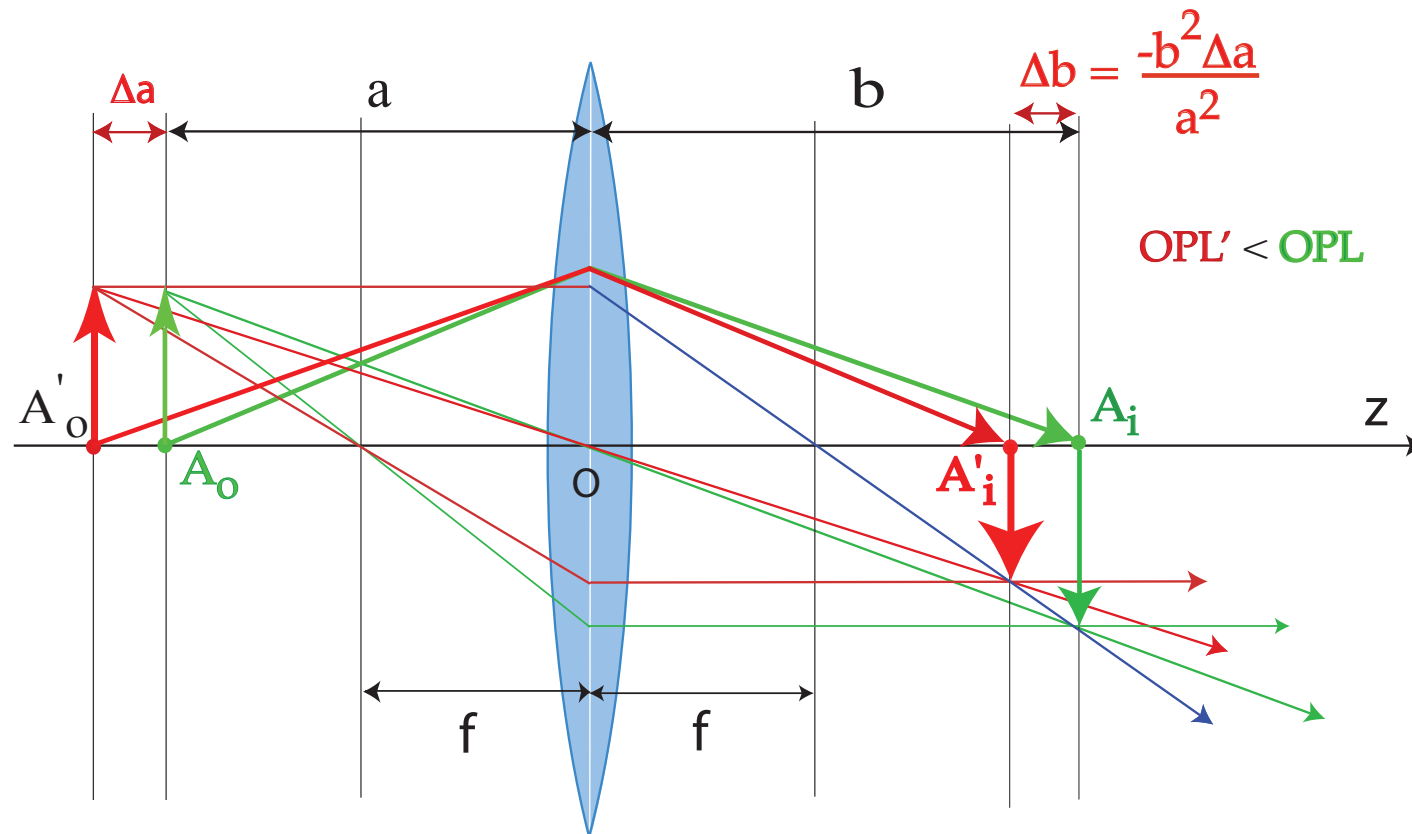
# OPD: underfocus



Underfocus weakens the objective lens, i.e. increases  $f$ . As a consequence the OPL from  $A_o$  to  $A'_i$  is larger:

$$e^{2\pi i \frac{\Delta f \lambda (\vec{q} \cdot \vec{q})}{2}}$$

# OPD: eccentricity



On the contrary keeping  $f$  constant and moving the object by  $\Delta a$  decreases the OPL.

$$T(\vec{q}) = e^{i\chi(\vec{q})} = \cos(\chi(\vec{q})) + i \underbrace{\sin(\chi(\vec{q}))}_{\text{Contrast transfer function}}$$

$$\chi(\vec{q}) = \pi \left[ W_{20} \lambda (\vec{q} \cdot \vec{q}) + W_{40} \frac{\lambda^3 (\vec{q} \cdot \vec{q})^2}{2} + \dots \right]$$

Where:

- ▶  $W_{20}$  : defocus ( $z$ )
- ▶  $W_{40}$ : spherical aberration ( $C_s$ )

At present TEM and STEM aberration correctors only correct axial aberrations, i.e. aberrations that affect images of point sources located on the optical axis.



# Wavefront aberrations to 6<sup>th</sup> order (cartesian coordinates)

$\{z, \pi (u^2 + v^2) \lambda\}$  (*defocus*)

$\{W(1, 1), 2\pi(u \cos(\phi(1, 1)) + v \sin(\phi(1, 1)))\}$

$\{W(2, 2), \pi\lambda((u - v)(u + v) \cos(2\phi(2, 2)) + 2uv \sin(2\phi(2, 2)))\}$

$\{W(3, 1), \frac{2}{3}\pi (u^2 + v^2) \lambda^2 (u \cos(\phi(3, 1)) + v \sin(\phi(3, 1)))\}$

$\{W(3, 3), \frac{2}{3}\pi\lambda^2 (u(u^2 - 3v^2) \cos(3\phi(3, 3)) - v(v^2 - 3u^2) \sin(3\phi(3, 3)))\}$

$\{W(4, 0), \frac{1}{2}\pi (u^2 + v^2)^2 \lambda^3\}$  (*3<sup>rd</sup> order spherical aberration or C<sub>3</sub>*)

$\{W(4, 2), \frac{1}{2}\pi (u^2 + v^2) \lambda^3 ((u - v)(u + v) \cos(2\phi(4, 2)) + 2uv \sin(2\phi(4, 2)))\}$

$\{W(4, 4), \frac{1}{2}\pi\lambda^3 ((u^4 - 6v^2u^2 + v^4) \cos(4\phi(4, 4)) + 4u(u - v)v(u + v) \sin(4\phi(4, 4)))\}$

$\{W(5, 1), \frac{2}{5}\pi (u^2 + v^2)^2 \lambda^4 (u \cos(\phi(5, 1)) + v \sin(\phi(5, 1)))\}$

$\{W(5, 3), \frac{2}{5}\pi (u^2 + v^2) \lambda^4 (u(u^2 - 3v^2) \cos(3\phi(5, 3)) - v(v^2 - 3u^2) \sin(3\phi(5, 3)))\}$

$\{W(5, 5), \frac{2}{5}\pi\lambda^4 (u(u^4 - 10v^2u^2 + 5v^4) \cos(5\phi(5, 5)) + v(5u^4 - 10v^2u^2 + v^4) \sin(5\phi(5, 5)))\}$

$\{W(6, 0), \frac{1}{3}\pi (u^2 + v^2)^3 \lambda^5\}$  (*5<sup>th</sup> order spherical aberration or C<sub>5</sub>*)

$\{W(6, 2), \frac{1}{3}\pi (u^2 + v^2)^2 \lambda^5 ((u - v)(u + v) \cos(2\phi(6, 2)) + 2uv \sin(2\phi(6, 2)))\}$

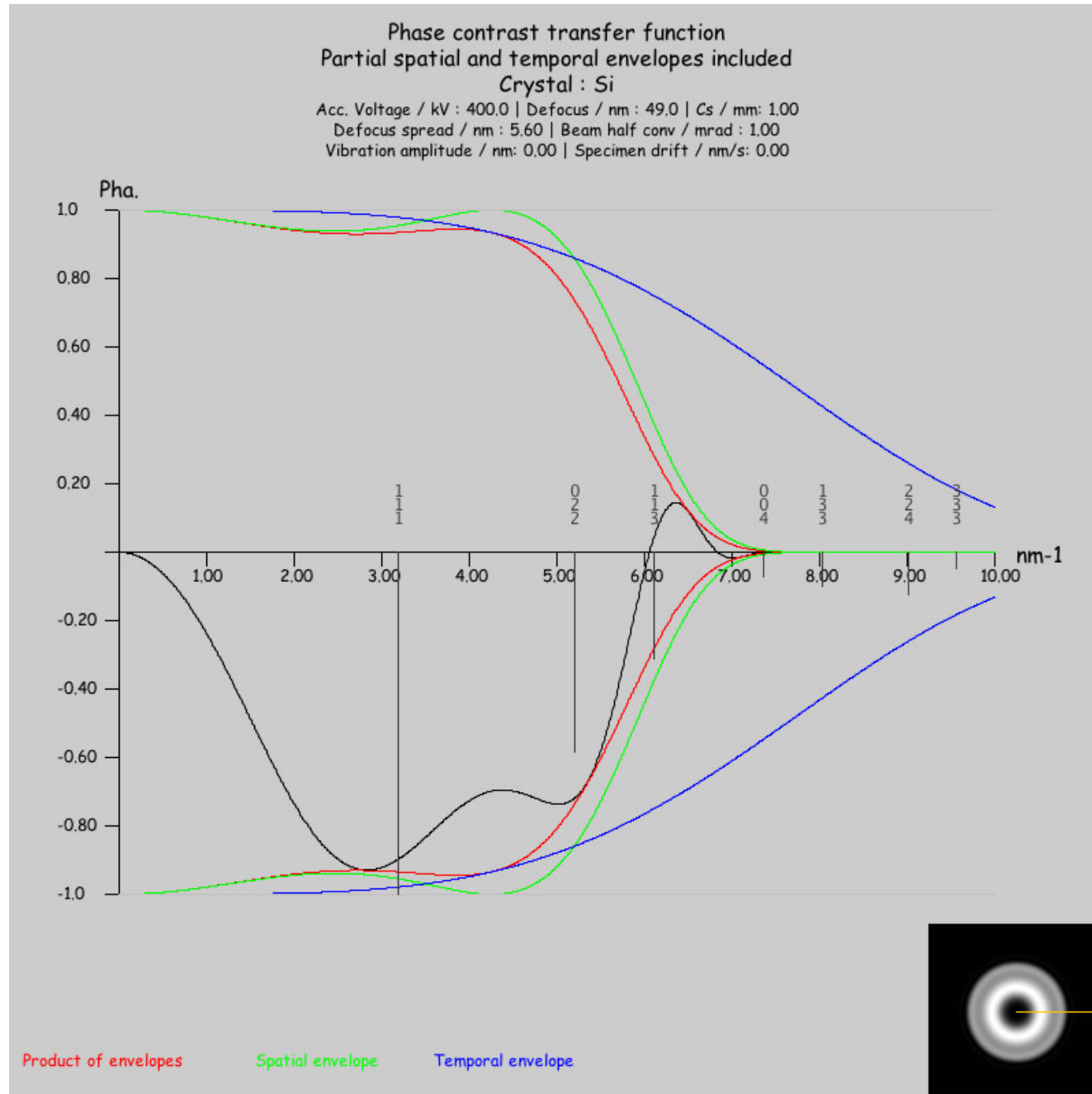
$\{W(6, 4), \frac{1}{3}\pi\lambda^5 ((u^6 - 5v^2u^4 - 5v^4u^2 + v^6) \cos(4\phi(6, 4)) + 4uv(u^4 - v^4) \sin(4\phi(6, 4)))\}$

$\{W(6, 6), \frac{1}{3}\pi\lambda^5 ((u^6 - 15v^2u^4 + 15v^4u^2 - v^6) \cos(6\phi(6, 6)) + 2uv(3u^4 - 10v^2u^2 + 3v^4) \sin(6\phi(6, 6)))\}$

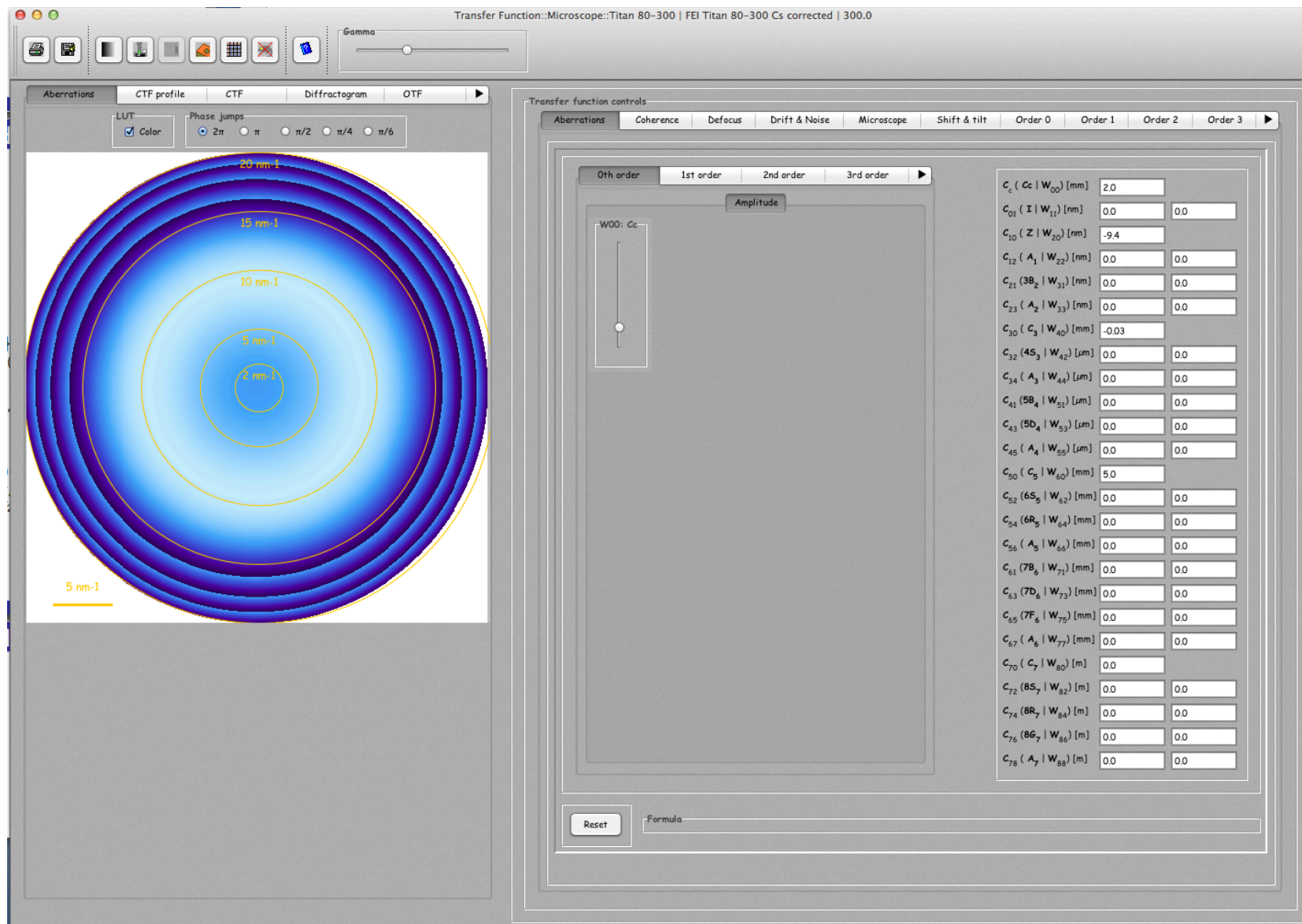
jems describes wavefront aberrations to order 8<sup>15</sup>.

<sup>15</sup>[http://cimewww.epfl.ch/people/stadelmann/jemsse/jemssev4\\_1520u2014.htm](http://cimewww.epfl.ch/people/stadelmann/jemsse/jemssev4_1520u2014.htm)

# Image formation: transfer function



# Plotting the transfer function



## Thickness series

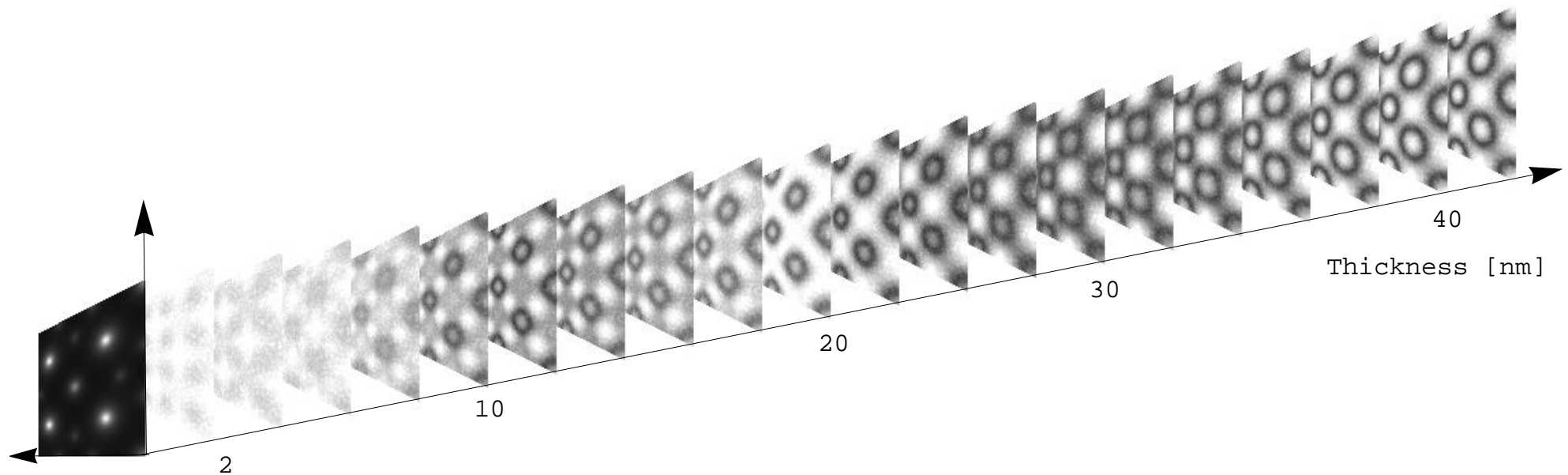


**Figure:** For a very small crystal thickness, a positive  $C_s$  objective lens and optimal defocus the atomic columns position appear as black dots in HRTEM (Weak Phase Object Approximation).

Increasing the crystal thickness makes the HRTEM images less straight forward to interpret. In high symmetry zone axis orientation, the electrons channel along the atomic columns and images present contrasts not correlated to them.

# HRTEM maps: comparaison MS-BW

HRTEM images map are usually calculated in order to figure out how images vary with defocus and crystal thickness.

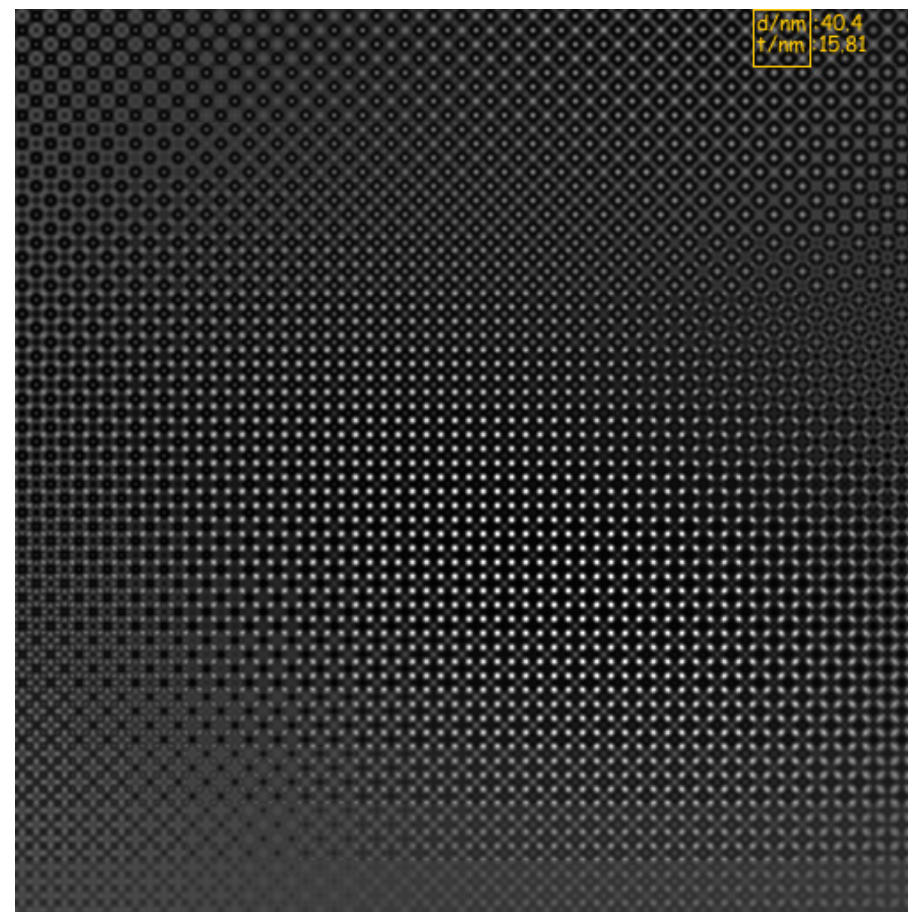


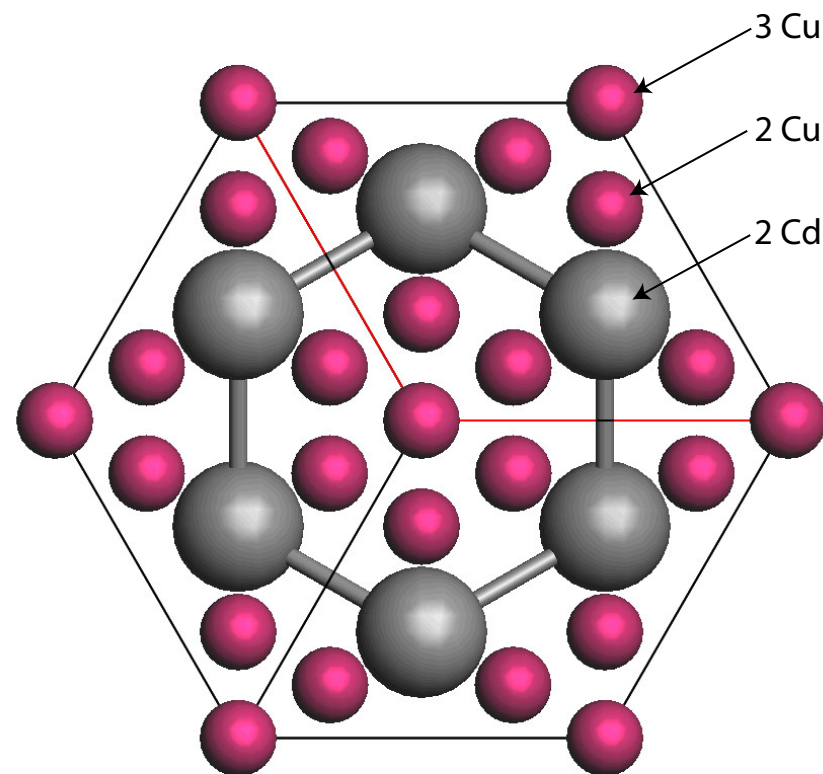
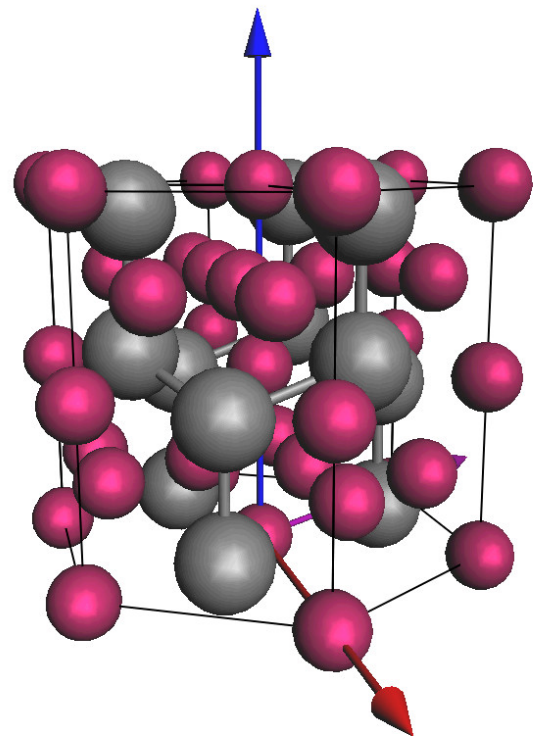
Figure:  $Fe_3S_4$  HREM map Bloch-wave method (1 + 436 BW)

Figure:  $Fe_3S_4$  HREM map multislice method (256x256).

HRTEM image maps calculated with either *multislice* or *bloch-wave* methods are identical.

# Why performing HRTEM simulation with aberration $C_s$ and $C_c$ corrections?

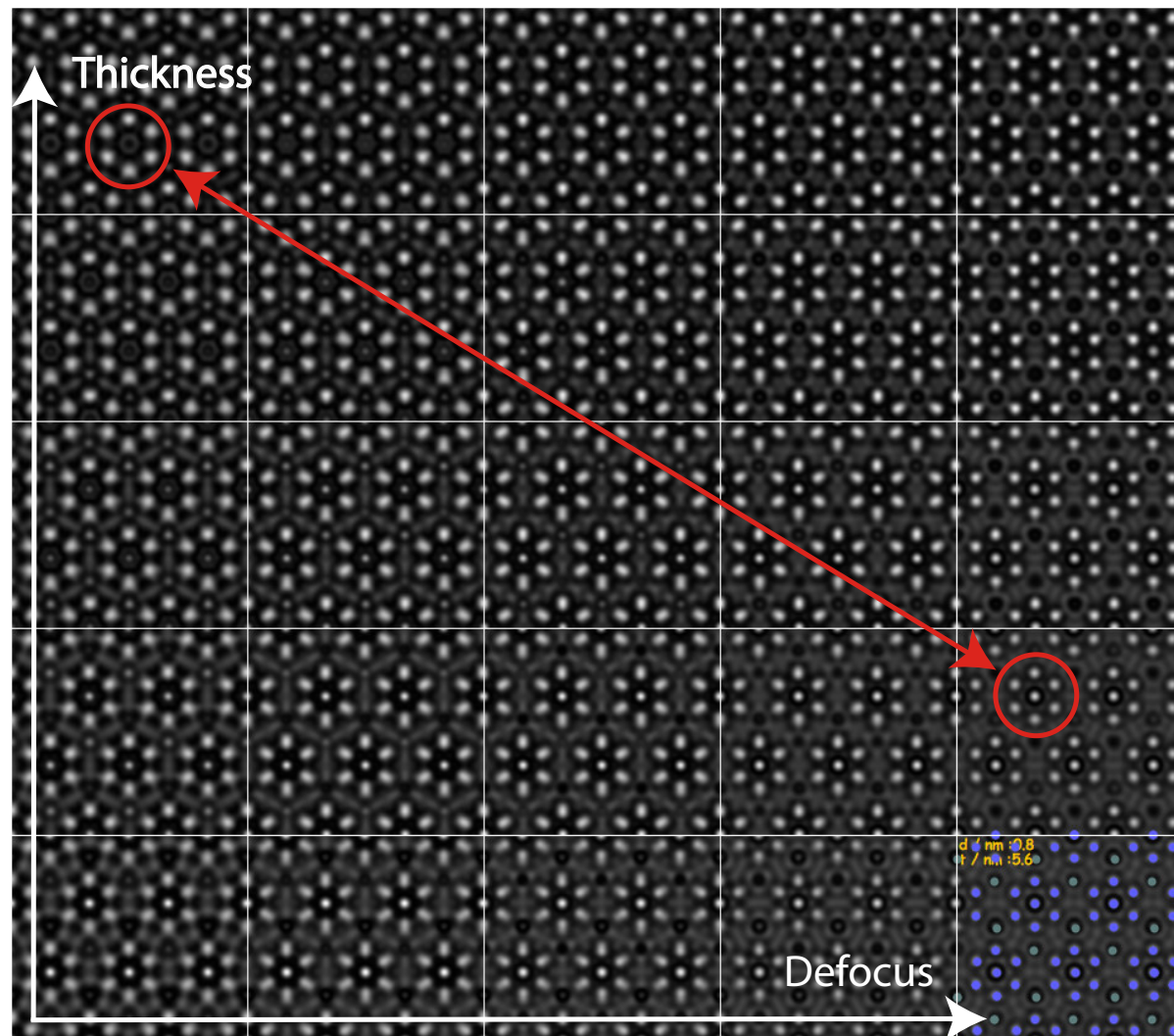
Example:  $CdCu_2$ , visibility of the 3 Cu atomic columns.



## *HRTEM image simulation conditions*

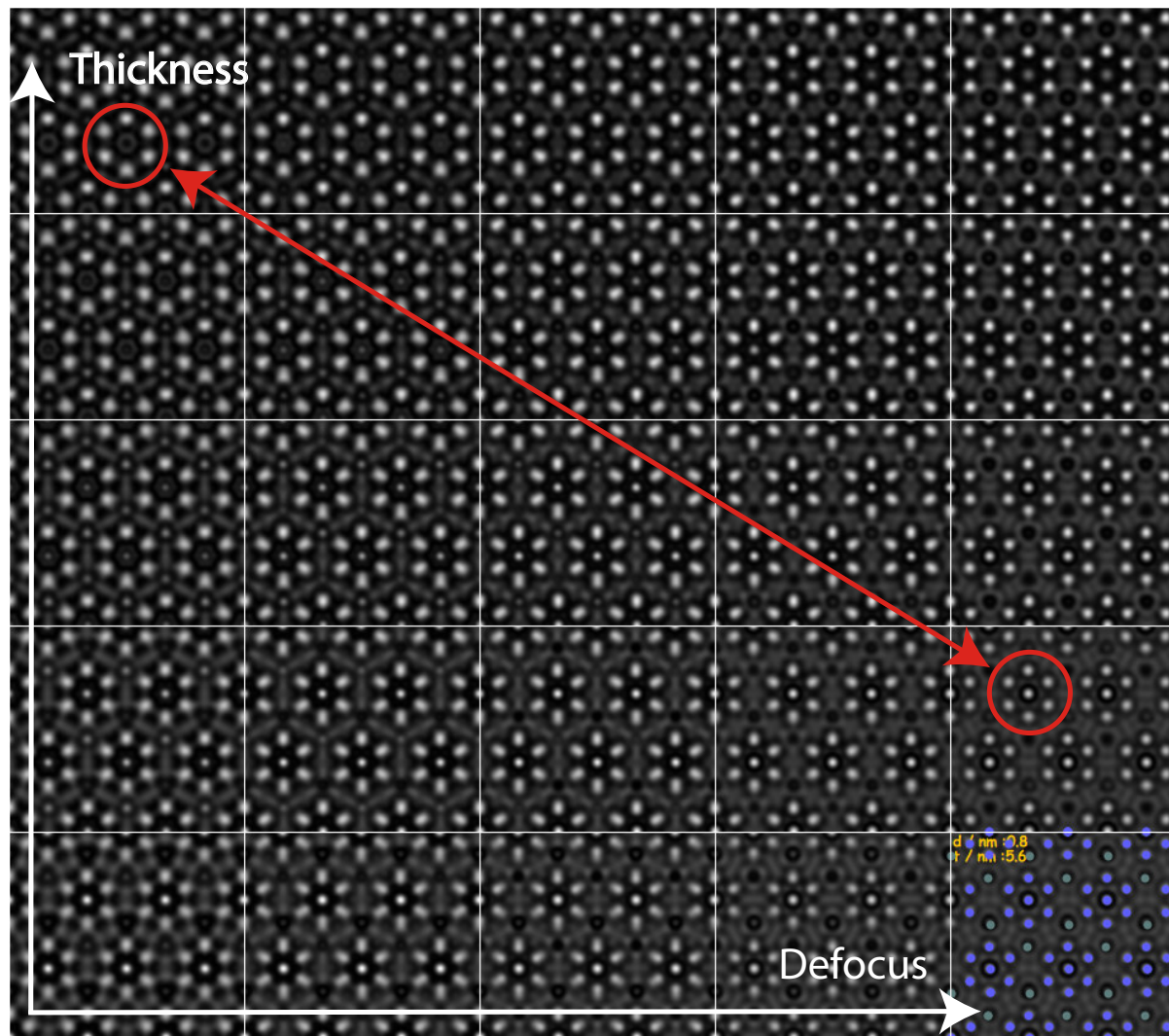
Acc. [kV]	$C_s$ [mm]	$C_5$ [mm]	$C_c$ [mm]	$\Delta E$ [eV]	Z [nm]	$\Delta z$ [nm]
300	-0.008	30	0.5	0.6	-4.9	1
300	-0.008	30	0.1	0.2	-2.0	1

Dynamical scattering effects are not affected by  $C_s$  and/or  $C_c$  corrected TEM!



Visibility of 3 Cu atomic columns depends on specimen thickness and defocus.

# $CdCu_2[001]$ : imaging parameters set 2



Improving  $C_c$  and  $\Delta E$  does not affect the visibility of 3 the Cu atomic columns depends on specimen thickness and defocus.

Visibility of the 3 Cu atomic columns is affected dynamical scattering (1 MeV  $C_s$  and  $C_c$  TEM).



# Detector MTF: Gatan 1K x 1K CCD

To make quantitative comparison with experimental HRTEM images the MTF of the detector must be introduced in the simulation.

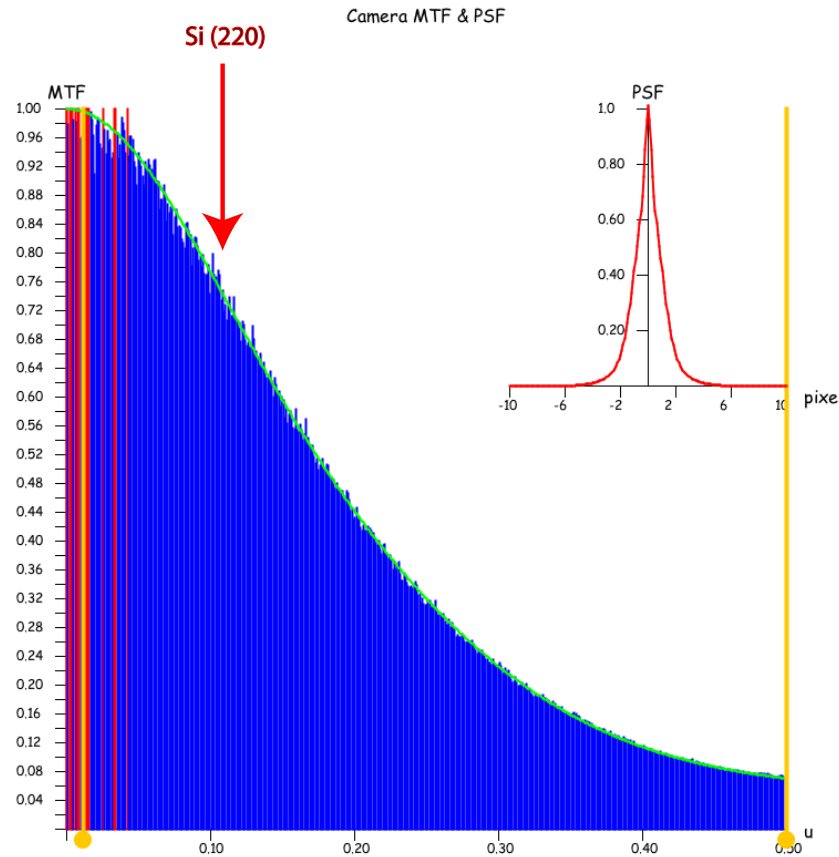


Figure: At high magnification Si (220) planes imaged with high contrast.

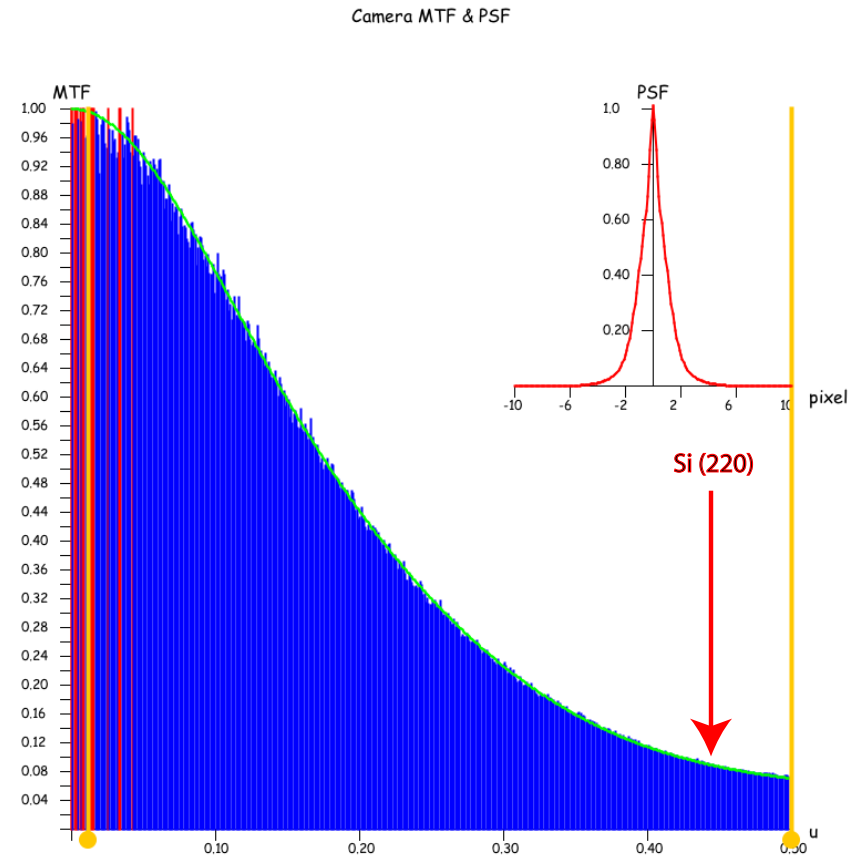


Figure: At low magnification Si (220) planes imaged with low contrast.

For quantitative comparison always use highest magnification!

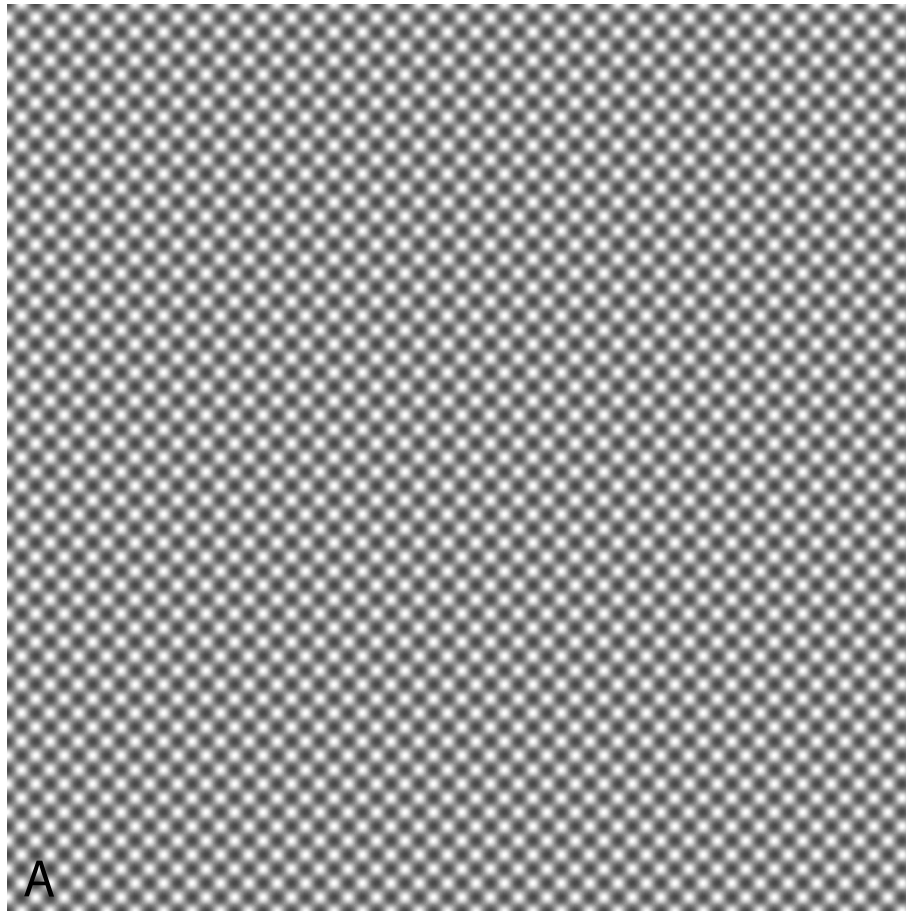


Figure: A: Si [001] simulation.

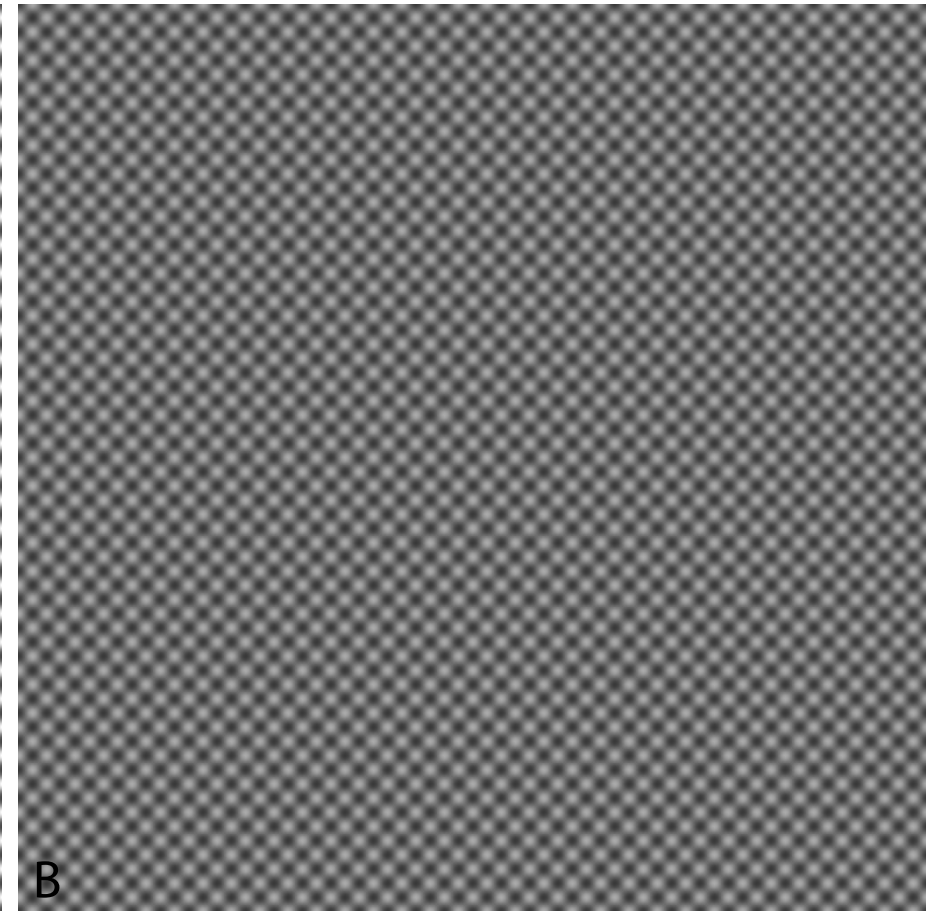


Figure: B: Si [001], simulation + CCD MTF.

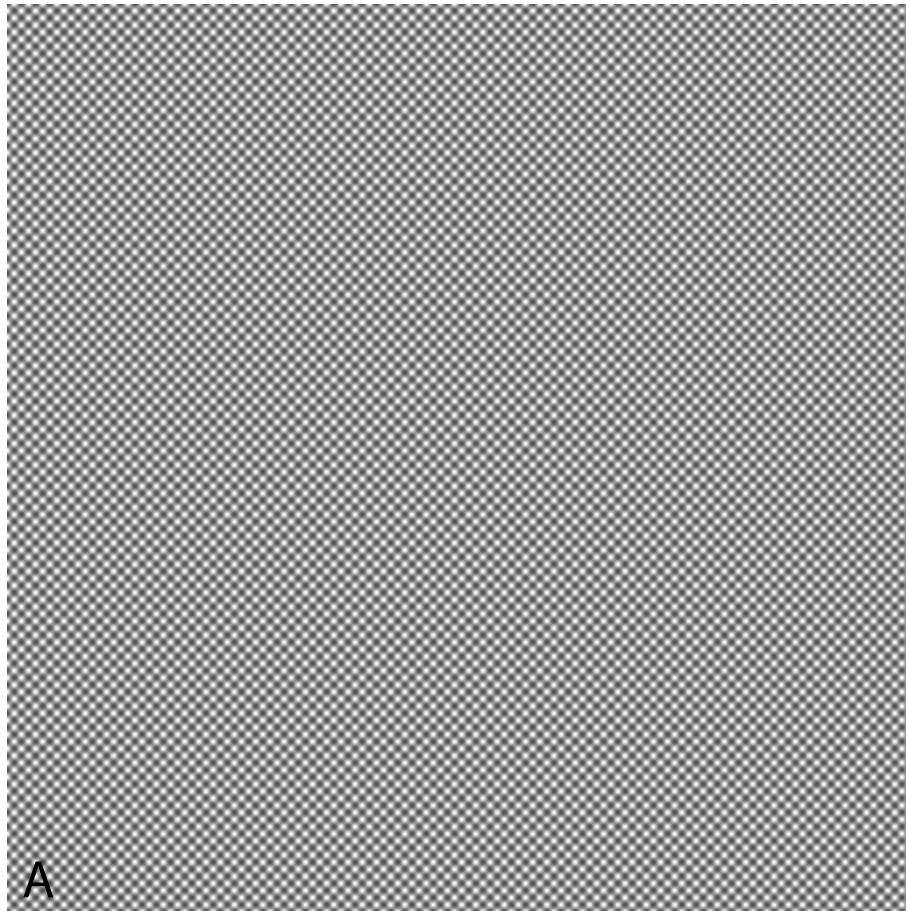


Figure: A: Si [001] simulation.

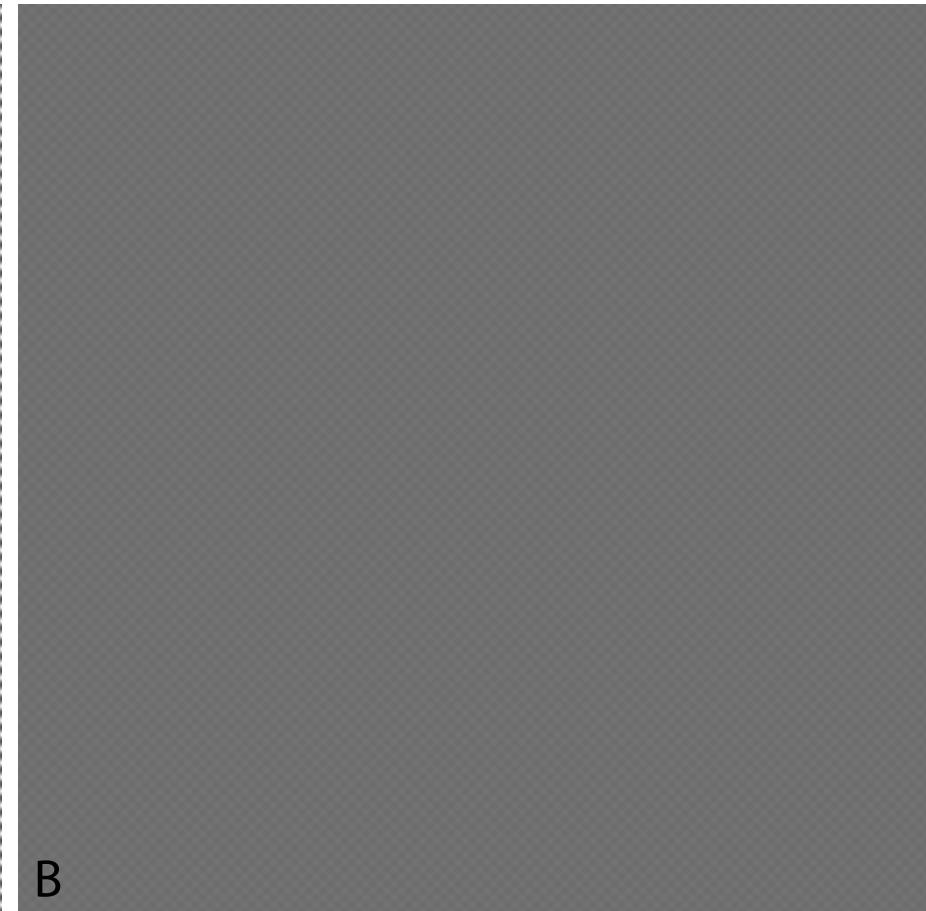


Figure: B: Si [001], simulation + CCD MTF.

# JEMS: STEM probe formation and aberrations

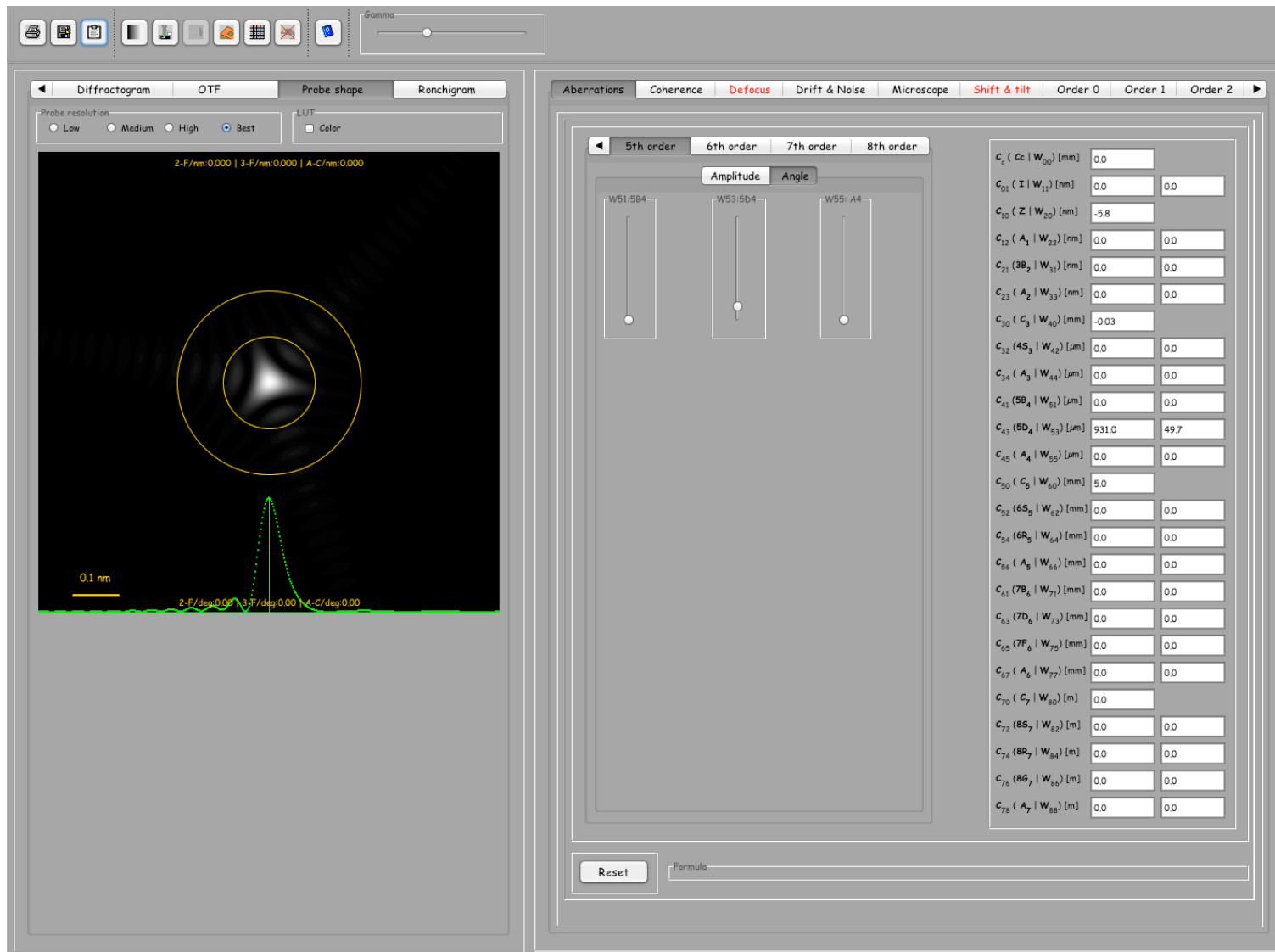


Figure: STEM probe with  $C_{43}$  geometrical aberration (Krivanek) or  $W_{53}$  wavefront aberration or 4th order three-lobe (Haider).

High Angle Annular Dark Field (HAADF): inelastically scattered electrons. How to simulate images?

Various approximations:

- ▶ Simple projected + convolution with probe intensity: no channeling effect (WPOA).
- ▶ Multislice calculation: channeling + inelastic scattering (absorption potential) + convolution with probe intensity.
- ▶ Frozen phonons approximation: atoms of super-cell displaced out of equilibrium position<sup>16</sup>, probe scanned on imaged area, intensity collected by annular detector.
- ▶ Ishizuka: ...
- ▶ Shiojiri:...
- ▶ ....

Except the first 2 methods, simulation time expensive. Approximations may suffice...

<sup>16</sup><file:///localhost/Applications/jemsMacOSX/html/graphene/ap.html>

# Approximations for HAADF: graphene

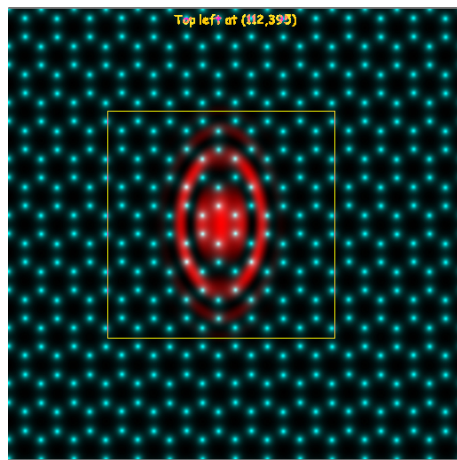


Figure: Probe affected by 2 fold astigmatism.

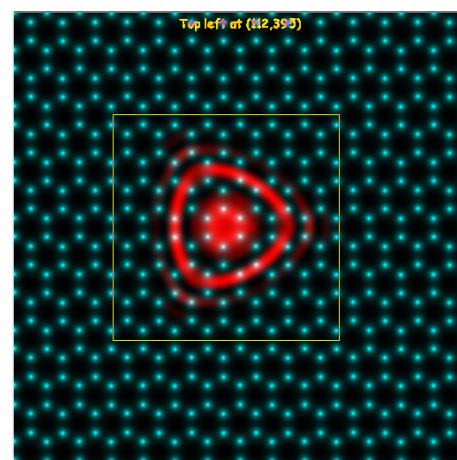


Figure: Probe affected by 3 fold astigmatism.

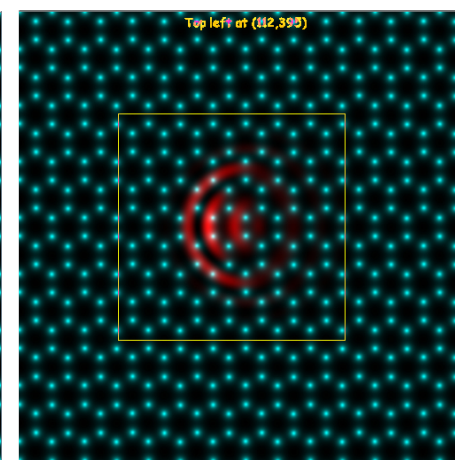


Figure: Probe affected by coma.

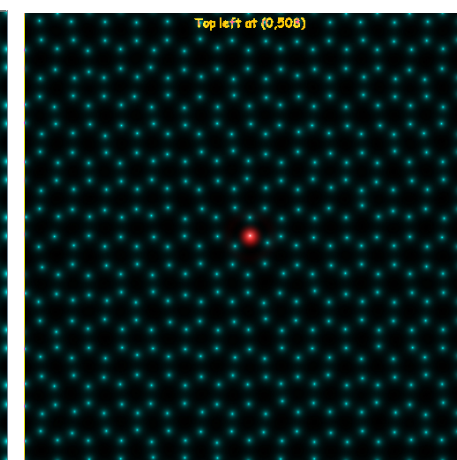


Figure: Corrected probe (best defocus).

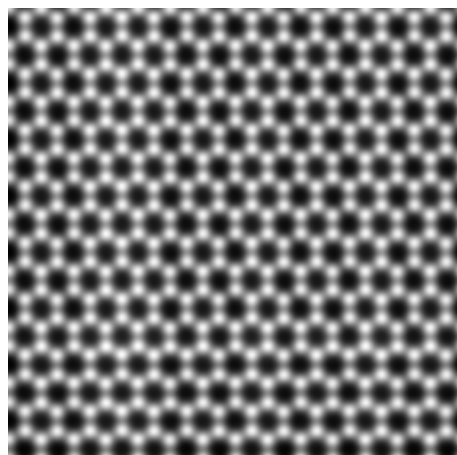


Figure: HAADF projected potential approximation.

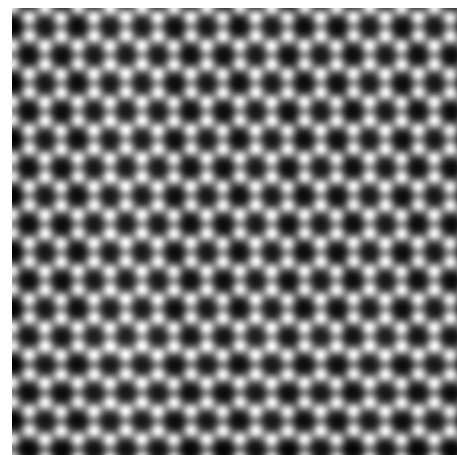


Figure: HAADF multislice calculation (simple).

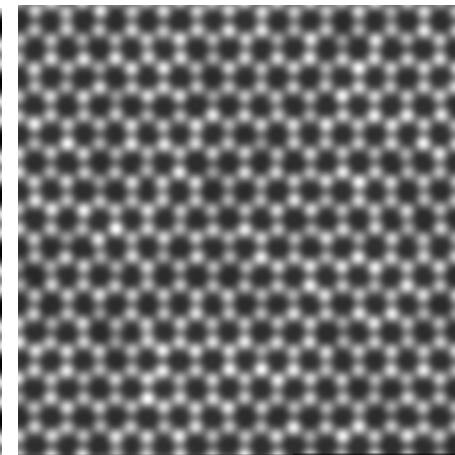


Figure: Frozen phonons 5 configurations.

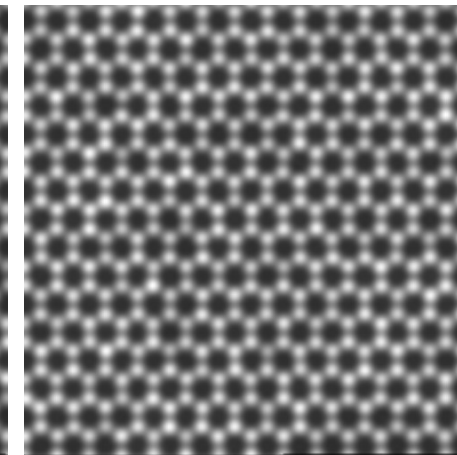


Figure: Frozen phonons 10 configurations.

# How to master HR(S)TEM image formation?

Read books and use an image simulation program (jems?)

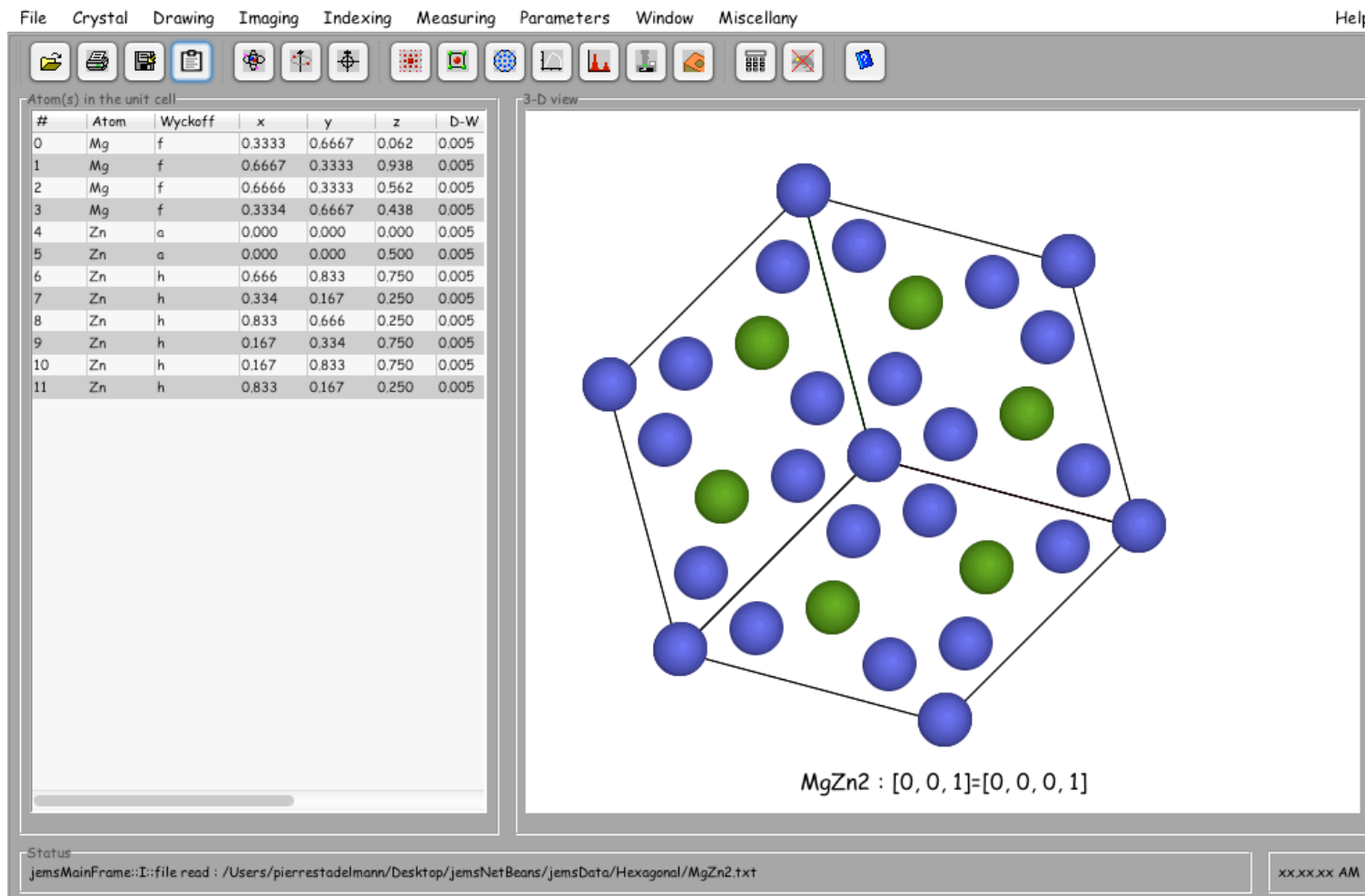


Figure: jems allows to perform many image simulations. The student edition is freely downloadable and ready for Mac OS, Windows XP, 7 or 8.1 and Linux ubuntu 64 bits.

<http://www.jems-saas.ch/>

# jems imaging features

jems allows changing most of the important imaging parameters in real time: coherence, aberrations to order 8, electronic noise, vibrations, drift, illumination and crystal tilts, magnification, ...

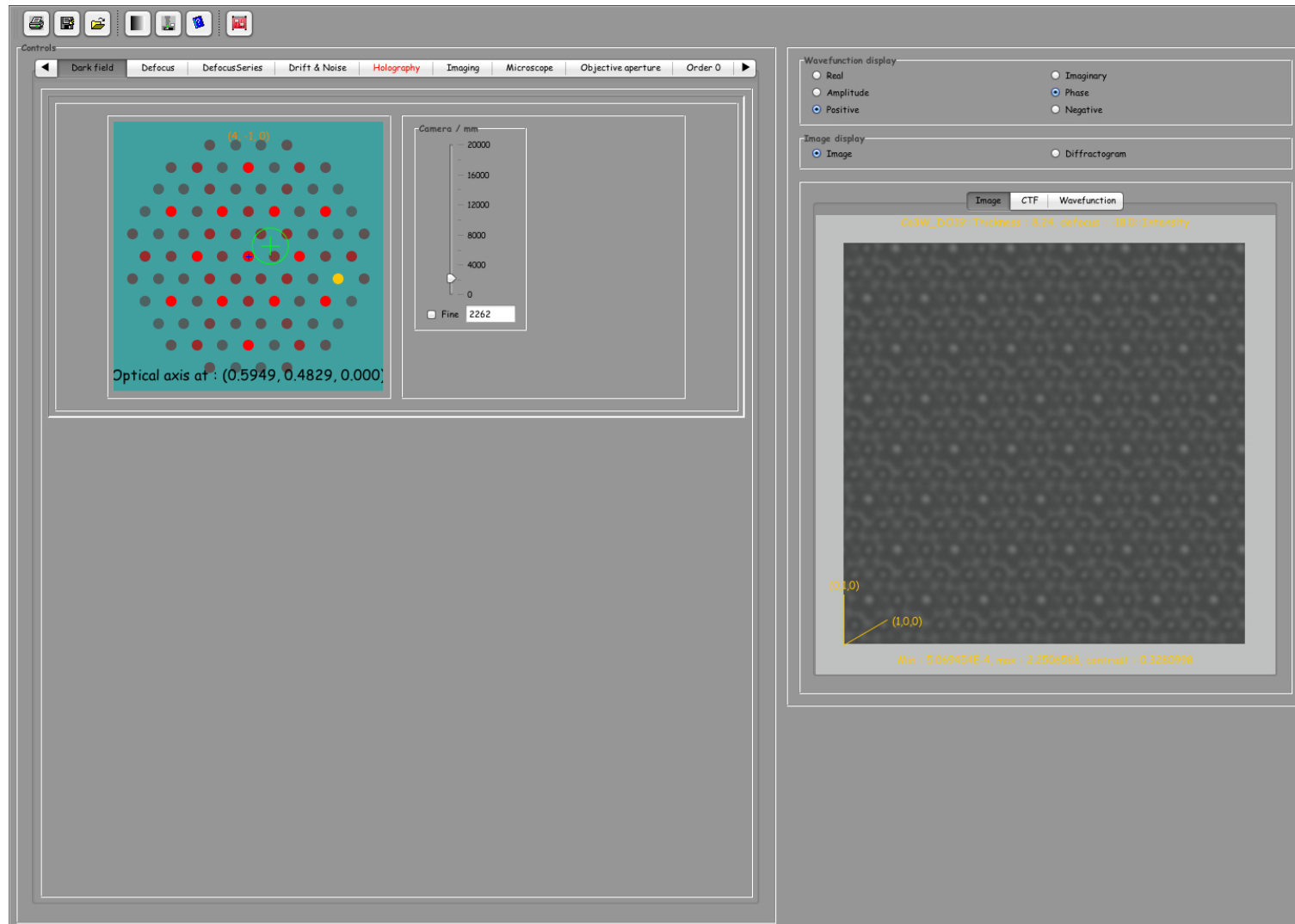


Figure: Looking at the effects of illumination tilt on HRTEM images.



**Please have jems installed on your PC or Mac before the lab. I can provide jems on USB keys in case you can't download it.**

`http://www.jems-saas.ch/`